FRICTION REDUCTION IN CO-AXIAL CATHETER SYSTEMS

by

Mark Davis

A thesis submitted to the faculty of
The University of Utah
in partial fulfillment of the requirements for the degree of

Master of Science

Department of Bioengineering
The University of Utah

December 1983

THE UNIVERSITY OF UTAH GRADUATE SCHOOL

SUPERVISORY COMMITTEE APPROVAL

of a thesis submitted by

Mark William Davis

This thesis has been read by each member of the following supervisory committee and by majority vote has been found to be satisfactory.

Joseph D. Andrade

Dennis L. Coleman

Alan F. Toronto

THE UNIVERSITY OF UTAH GRADUATE SCHOOL

FINAL READING APPROVAL

To the Graduate Council of The University of Utah:

I have read the thesis of Mark William Davis in its final form and have found that (1) its format, citations, and bibliographic style are consistent and acceptable; (2) its illustrative materials including figures, tables, and charts are in place; and (3) the final manuscript is satisfactory to the Supervisory Committee and is ready for submission to the Graduate School.

Date

Joseph D. Andrade
Supervisory Committee

Approved for the Major Department

Joseph D. Andrade
Chairman Dean

Approved for the Graduate Council

James L. Clay
Dean of The Graduate School

ABSTRACT

The purpose of these experiments was to evaluate the effectiveness of treating manufactured catheters with a radio-frequency induced plasma to obtain decreased static and dynamic friction between treated and nontreated catheters. This was accomplished by treating the catheters for 0, 5, 30, 120 and 300 seconds and inserting the treated catheter through the lumen of a larger diameter, nontreated catheter, around a loop, and measuring the force required to initiate and maintain movement of the inner catheter through the secured outer catheter.

Silicone rubber, polyethylene and two different polyurethanes were studied dry and in three different fluid media: wetted, hydrated in a physiologically buffered saline, and in a 10 mg/ml albumin solution. X-ray photoelectron spectroscopy was performed on all dry catheters to determine surface chemical composition before and after radio frequency glow discharge treatment. Water contact angles were obtained on all dry catheters to determine the hydrophobic/hydrophilic nature of the catheters before and after treatment. Microscopic evaluation and infra-red absorption studies were also performed on some catheters to correlate results. A short in-vivo study was initiated to obtain qualitative results of the catheter treatments.

No correlation between radio-frequency glow discharge treatment times and friction was observed. Earlier studies of this type showed some decrease in friction with radio frequency glow discharge treatment, although these previous tests were performed on pure materials and not on manufactured catheters as was done in these experiments. There was a definite correlation found between the fluid media used and the friction observed. These findings varied depending on the catheter materials utilized. Further study is necessary to evaluate the basis behind these findings.

TABLE OF CONTENTS

Page

ABSTRACT iv

LIST OF TABLES viii

LIST OF FIGURES ix

ACKNOWLEDGEMENTS xii

Chapter

1. INTRODUCTION 1

2. BACKGROUND 5

2.1 Catheter Materials 5

2.1.1 Polyethylene 6
2.1.1 Polyurethane 6
2.1.3 Silicone Rubber 8

2.2 Plasma Treatment 9

2.3 Friction 11

3. MATERIALS AND METHODS 14

3.1 Materials 14

3.1.1 Polyurethane 1 14
3.1.2 Polyurethane 2 15
3.1.3 Silicone Rubber 15
3.1.4 Polyethylene 16

3.2 Methods 16

3.2.1 Preparation of Materials 16
3.2.2 Radio Frequency Glow Discharge . . 17
3.2.3 X-ray Photoelectron Spectroscopy . 20
3.2.4 Contact Angle 22
3.2.5 Friction 25
3.2.6 Infrared Spectroscopy 28
3.2.7 Mechanical Tests 29
3.2.8 In-vivo Tests 29

Page

4. RESULTS AND DISCUSSION 31

4.1 X-ray Photoelectron Spectroscopy 31

4.1.1 Polyurethane 1 31
4.1.2 Polyurethane 2 39
4.1.3 Silicone Rubber 42

4.2 Contact Angle 47

4.2.1 Polyurethane 1 47
4.2.2 Polyurethane 2 51
4.2.3 Silicone Rubber 51
4.2.4 Conclusions 52

4.3 Friction 53

4.3.1 Discussion 53
4.3.2 Polyethylene-Polyurethane 1 59
4.3.3 Polyethylene-Polyurethane 2 62
4.3.4 Polyethylene-Silicone Rubber . . . 62
4.3.5 Polyurethane-Polyurethane 1 67
4.3.6 Polyurethane-Polyurethane 2 70
4.3.7 Polyurethane-Silicone Rubber . . . 70
4.3.8 Conclusions 75

4.4 Mechanical Tests 80

4.5 In Vivo Tests 81

5. CONCLUSIONS AND RECOMMENDATIONS FOR FUTURE WORK 83

REFERENCES 87

LIST OF TABLES

Table		Page
4.1	X-ray photoelectron spectroscopy derived atomic percent compositions at control, 5, 30, 120 and 300 seconds for Ducor polyurethane, B-D polyurethane and silicone rubber catheters	32
4.2	Full width at half maximum and peak binding energies obtained with X-ray photoelectron spectroscopy for elemental C, O, N on PU_1 and PU_2 and C, O, Si on SR shown at RFGD treatment times of 0, 5, 30, 120 and 300 seconds	38
4.3	Advancing and receding water contact angles for PU_1, PU_2 and SR at radio frequency glow discharge treatment times of 0, 5, 30, 120 and 300 seconds	48
4.4	Friction values for the catheter pairs PE-PU_1, PE-PU_2, PE-SR, PU-PU_1, PU-PU_2, and PU-SR for radio frequency glow discharge treatment times of 0, 5, 30, 120 and 300 seconds. The average force, standard deviation and average maximum value for three tests per catheter pair is given. The friction values for each catheter pair are given for four different solutions	58

LIST OF FIGURES

Figure		Page
3.1	Radio frequency glow discharge apparatus. A - End-on view of sample chamber with sample rack in center. B - Side view of sample chamber with sample rack. C - Side view of RFGD apparatus showing sample chamber, with sample rack, surrounded by RF coils	18
3.2	Schematic representation of the radio frequency glow discharge apparatus used in this study	19
3.3	Apparatus used for determination of contact angles by the Wilhelmy plate method. A - H-P X-Y recorder. B - Electrobalance. C - Crosshead. D - Sample platform. E - Beaker for distilled water	24
3.4	Illustration showing determination of values used for determining contact angles with the Wilhelmy Plate method	25
3.5	Apparatus used in the determination of friction values. An outer catheter is placed under pulleys, wrapped around the loop, and placed under the opposite pulley. The inner catheter is fed through the outer catheter and attached to a mechanical tester .	26
4.1	Carbon-to-oxygen ratios versus radio frequency glow discharge time for the Ducor polyurethane, PU_1	33
4.2	Effect of radio frequency glow discharge treatment on the urea carbon of the Ducor polyurethane shifted 4.0 eV from the main aliphatic carbon for the untreated, 5, 30, 120 and 300 second treated materials	35
4.3	The O-1s spectra of the untreated Ducor polyurethane, PU_1, showing resolution of two peaks at 2.0 eV separation with a 1:1 ratio .	37

Figure		Page
4.4	Carbon-to-oxygen ratios vs. radio-frequency glow discharge times for the Becton-Dickinson polyurethane, PU_2	40
4.5	Atomic percent of C, O, Si as a function of radio-frequency glow discharge treatment time for the silicone rubber catheter	44
4.6	The Si-2p spectra versus radio frequency glow discharge treatment time for the silicone rubber catheter. A - Untreated. B - 30 second treated. C - 120 second treated. D - 300 second treated	45
4.7	Advancing water contact angle as a function of radio-frequency glow discharge treatment time for the treated inner catheters; polyurethane 1, polyurethane 2 and silicone rubber	49
4.8	Receding water contact angle as a function of radio-frequency glow discharge treatment time for the treated inner catheters; polyurethane 1, polyurethane 2 and silicone rubber	50
4.9a,b	Representative graphs produced by friction types "A" and "B." (See text for description.)	54
4.9c,d, e	Representative graphs produced by friction types "C," "D," and "E." (See text for description.)	56
4.10	Friction as a function of radio frequency glow discharge treatment time for the polyethylene-Ducor polyurethane catheter pair, $PE\text{-}PU_1$	60
4.11	Friction as a function of the fluid media for the polyethylene-Ducor polyurethane catheter pair, $PE\text{-}PU_1$	61
4.12	Friction as a function of the radio-frequency glow discharge treatment time for the polyethylene-B-D polyurethane catheter pair, $PE\text{-}PU_2$	63
4.13	Friction as a function of the fluid media for the polyethylene-B-D polyurethane catheter pair, $PE\text{-}PU_2$	64

Figure		Page
4.14	Friction as a function of the radio-frequency glow-discharge treatment time for the polyethylene-silicone rubber catheter pair, PE-SR	65
4.15	Friction as a function of the fluid media for the polyethylene-silicone rubber catheter pair, PE-SR	66
4.16	Friction as a function of the radio frequency glow discharge treatment time for the Ducor polyurethene-Ducor polyurethane catheter pair, PU-PU_1	68
4.17	Friction as a function of the fluid media for the Ducor polyurethane-Ducor polyurethane catheter pair, PU-PU_1	69
4.18	Friction as a function of the radio-frequency glow discharge treatment time for the Ducor polyurethane-B-D polyurethane catheter pair, PU-PU_2	71
4.19	Friction as a function of the fluid media for the Ducor polyurethane-B-D polyurethane catheter pair, PU-PU_2	72
4.20	Friction as a function of the radio-frequency glow discharge treatment time for the Ducor polyurethane-silicone rubber catheter pair, PU-SR	73
4.21	Friction as a function of the fluid media for the Ducor polyurethane-silicone rubber catheter pair, PU-SR	74

ACKNOWLEDGEMENTS

The author would like to extend appreciation and thanks to Dr. Dennis Coleman, Dr. Alan Toronto and primarily Dr. Joseph Andrade for the help, support and especially patience in this effort. Special thank you to Dr. Lee Smith for all the invaluable time given in aid and preparation of necessary support material. Thank you to Dr. Frank Miller for financial and academic support in the dog studies; Mr. Vince De Caprio from Becton-Dickinson for polyurethene catheters; Cordis catheter company for their financial support in the characterization studies; Cook catheter company; and those in the Bioengineering department who made my experience at the University of Utah enjoyable.

CHAPTER 1

INTRODUCTION

The use of catheters as a diagnostic tool for the clinical physician has rapidly grown. Since the early days of catheterization, when, in 1929, Dr. Werner Forssmann advanced a ureteral catheter up his own antecubital vein to the right atrium of the heart and proceeded to walk up several flights of stairs to the X-ray department to document the achievement (1), the usefulness of such a tool was perceived. Although Dr. Forssmann's findings were not initially well received, in 1941 Cournand and Ranges (2) reported on a technique for catheterization of the right heart to aid in the understanding of the fundamental physiological problems existing in many forms of congenital and acquired heart disease.

Since these initial reports on catheterization there has been a steady increase in the clinical value of the data which may be obtained from not only cardiac catheterization but from other forms of catheterization. For example, angiography occupies a unique place in medicine as an invaluable aid in the diagnosis of diseases of the viscera, such as tumors. The damage to some arteries caused by atheromatous change is often reflected

in the arteriogram by injecting radiopaque dye into the artery via a catheter and observing variations in the structure of the artery (3).

Other applications of catheters include their use in long-term intravenous feeding (4,5) drug delivery to specific organs (6,7), monitoring local blood pressures (8,12), occlusion of blood vessels to decrease or eliminate blood flow to specific areas (13-15), to aid in the removal of gallstones and kidney stones (16), and "squashing" plaques with a balloon-tip catheter to clear blocked arteries (17). A well known, and widely used, catheter system developed in recent years is the Swan-Ganz catheter (18,19) which is used to monitor cardiovascular pressures through a balloon-tipped catheter which is advanced to the proper area by allowing the balloon to "float" in the vein. Other fairly recent developments include catheters with fiber optic aximeters, intracavitary phonocatheters and many others (18).

Complications are associated with the use of these catheter systems. Some major complications include myocardial infarctions during cardiac catheterization (20), air and fragment embolisms (21), cerebral and pulmonary ischemia (22), septic endocarditis (23), and mortality (24). Other complications include thrombus formation (25-27), infection (28-30), lost catheters (31), thrombophlebitis (32), hematoma (21), and even defective limb growth (33,34).

With all of the advances in catheter technology, one particular technique has recently evolved that deserves special attention; it is the coaxial catheter system (35) used for many practical clinical situations. Among these are the closure of the carotid cavernous fistulae, reduction of epistaxis, embolization of small tumors otherwise inaccessible with larger catheters, and possible reversible sterilization by occlusion of the fallopian tubes or testicular veins.

Another exciting development has been the use of these coaxial catheters as an option to surgical procedures on the coronary arteries on those patients with acute myocardial infarctions (36). A large outer catheter is advanced up the aorta and placed at the entrance to the coronary artery. A smaller inner catheter is inserted through the larger outer catheter into the coronary artery and located in proximity to the plaque occluding the vessel. Thrombolysin (streptokinase and plasmin) is subsequently administered to dissolve the plaque, thereby eliminating the obstruction of blood flow to the ischemic tissue.

One persistent and irritating problem inherent in the coaxial system is the friction encountered when the smaller, inner catheter is manipulated through the larger, outer catheter (37). Although this problem is not only due to polymer-polymer surface interaction, it has been shown

that various treatments of the polymer surface may reduce the inherent friction (38).

This investigation attempts to define the variables involved in the polymer-polymer interactions resulting in friction, and subsequently analyze attempts to reduce the friction by the use of a radio frequency glow discharge surface modification. Other possible techniques for friction reduction are briefly discussed.

CHAPTER 2

BACKGROUND

2.1 Catheter Materials

There are a vast number of polymers employed in the manufacturing of catheters. The most common of these include polyvinyl chloride (PVC), polyurethanes, polyethylene, polytetrafluoroethylene (Teflon) and silicone rubber. These catheters range from hard, rigid, steel-reinforced, large configurations to flaccid, elastomeric, small-diameter catheters.

Many commercially produced catheters contain additives to allow extrusion of the polymer as well as to provide stabilization of the finished product. These additives include antioxidants (39), ultraviolet (UV) stabilizers (40), plasticizers (41), processing aids (such as surface and internal lubricants) (39,42), and colorants or pigments (for aesthetic or optical purposes) (39). Fillers such as silica (sand), glass beads, or carbon fibers may be utilized to enhance mechanical properties or provide bulk to the material (39). There are also fillers such as heavy metal compounds added to furnish radiopacity.

Polyethylene, two types of polyurethanes, and silicone rubber were used in this study.

2.1.1 Polyethylene

Polyethylene is a homopolymer of ethylene produced by addition polymerization. Its backbone structure is: $\{CH_2\text{-}CH_2\}$. Two types of polyethylene are manufactured commercially, high-density polyethylene (HDPE) and low-density polyethylene (LDPE). The HDPE is a very linear polymer with very few side chains. It is usually 75% crystalline with a density of 0.955 to 0.970 g/cm^3 (38). Low-density polyethylene has a density of approximately 0.900 to 0.935 g/cm^3 (38) with extensive branching and is usually $\sim$ 50% crystalline. Low-density polyethylene is therefore much more suitable for catheter material since the lower degree of crystallinity means a less rigid material with better handling characteristics. The high-density polyethylene is used for applications wherein a very hard, rigid material is desired, e.g., acetabular socket for hip replacement. More about polyethylene can be found in Reference 43.

2.1.2 Polyurethane

Polyurethanes are complicated materials that vary dramatically in composition. Basically, a polyurethane is composed of three parts, a soft segment, a hard segment, and chain extenders. The soft segment of polyurethane is a polyol such as hydroxy-terminated polyester (e.g., polyethylene adipate, poly -caprolactone), polyether (e.g., polypropylene oxide, polytetramethylene gylcol), or other

polyols (e.g. hydroxy-terminated polybutadiene, polyisobutylene, fluorinated polyethers, polydimethyl siloxane (PDMSO), and phosphorous containing oligomers).

The hard segment is obtained with an excess of a difunctional isocyanate. The most commonly used diisocyanates are 4,4' diphenylmethane diisocyanate (MDI), hexamethylene diisocyanate (HDI), and 2,4 tolylene diisocyanate (TDI).

The chain extenders are of two types, a diol of diamine creating either a urethane

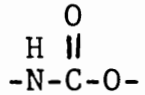

,

or a urea

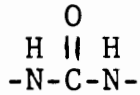

linkage. The general reaction for a diol-based urethane is shown in Equation 2.1 (44).

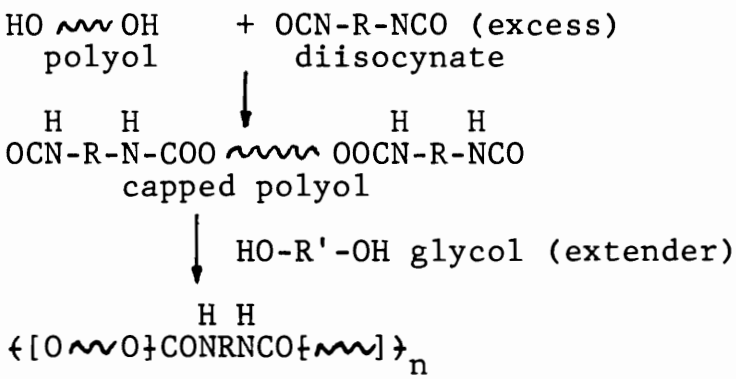

[2.1]

Thus, a segmented polyurethane block copolymer is produced. The above reaction results in a polydispersed block copolymer with an -OH/-NCO $\geq$1.0.

Urethanes with polyether polyols usually have better hydrolysis resistance and poorer oxidative stability than those with polyester soft blocks. Therefore, because of the environment in which they will be utilized, catheters are more frequently composed of polyether-type urethanes. As can be seen, a wide range of polyurethanes can be produced to meet specifications which match the desired final usage of the material.

2.1.3 Silicone Rubber

Silicone rubber is a polymer of dimethyl siloxane (PDMSO) with a backbone of:

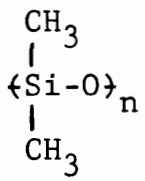

[2.2]

This polymer can be cross-linked to produce an elastomeric, more stable product. Medical-grade silicone rubbers are either room temperature vulcanized (RTV), whereby the polymer is vulcanized with reaction of two separate chemical components or reaction with air, or heat vulcanizing where heat is applied to overcome an activation energy (45).

One-component RTV silicones are vulcanized by a reaction with atmospheric water to release acetic acid and allow the cross-linking agent, triacetoxy silane

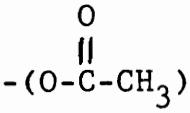

to be hydrolyzed. This leaves an hydroxy group in place of the acetate. The dimethyl siloxane with an hydroxy-terminated end reacts with the hydroxylated cross-linking agent, producing a vulcanized rubber. This is shown in Equation [2.3] (46).

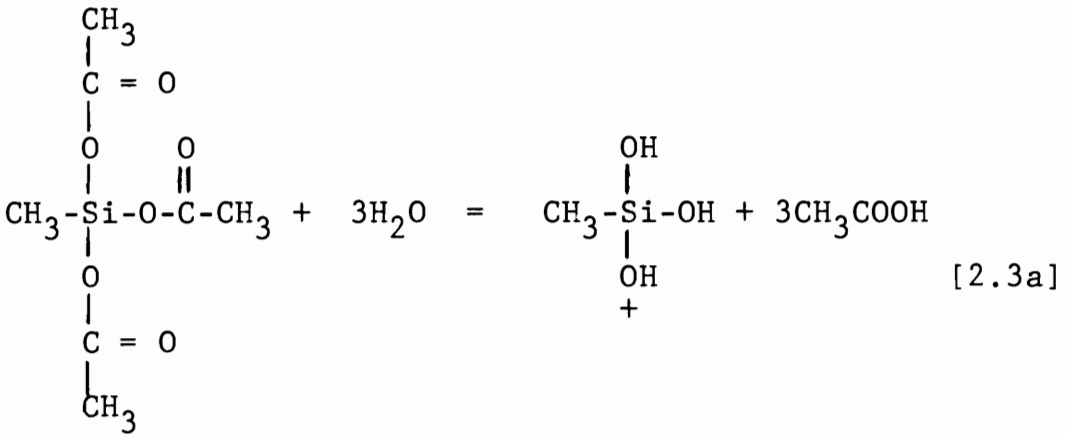

[2.3a]

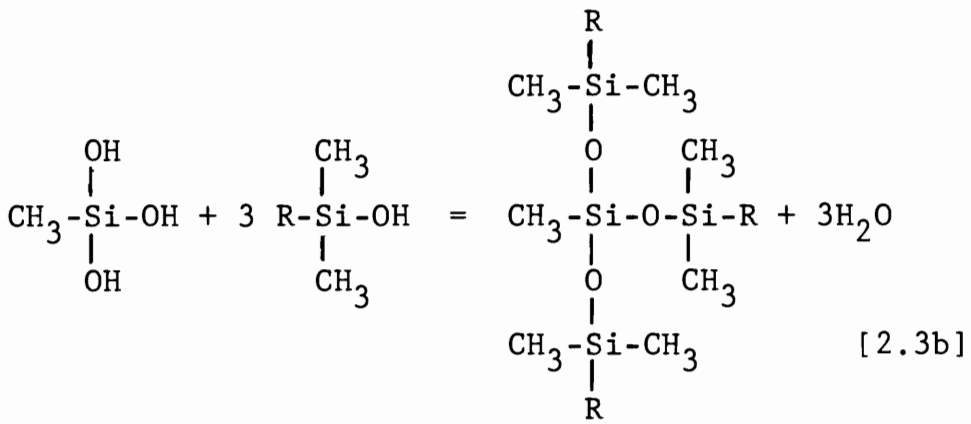

[2.3b]

2.2 Plasma Treatment

A plasma is defined as an unstable environment of ions, metastable electrons in excited states, atoms of a given gas and intense UV visible radiation. This plasma is created by supplying energy to a gaseous system under

partial vacuum. Two general methods are employed to supply energy to the system (47,48). The first is an electrode discharge system, the other uses radio frequency energy to create the plasma. The electrode system tends to run at high temperatures, which may be undesirable for many applications, especially with polymers. The radio frequency method is performed at ambient temperatures, which is usually more desirable. The gas used in the plasma is dependent upon the desired surface alteration. The most common gases used are either the inert gases (i.e., He, Ar), or a reactive gas (O_2, NH_3, H_2, etc.).

A plasma reacts with the surface of the polymer, thereby creating different or altered species on the surface. For example, Hollahan reports a massive hydroxylation of polymethylsiloxane surfaces upon treatment with oxidizing plasmas (49).

Westerdahl et al. concluded that the plasma only affects the top few molecular layers (50), although the depth of penetration of the plasma is a function of the power applied to the radio frequency as well as the duration of the discharge.

Calspan Corporation has used the technique of RFGD for sterilization of polymers (51). E. coli and bacillus stearothermophilus were deliberately incorporated into polymers and exposed to nine-minute treatments with the vacuum RFGD apparatus. The power setting was unspecified. Complete killing of the bacteria occurred.

A possible side effect of RFGD which could prove to be detrimental to polymers is photodegradation (52). Polymers containing no photostabilizers can be severely degraded by the ultraviolet light which is produced upon discharge. The light produced in the visible region is why the technique is termed "glow" discharge.

2.3 Friction

It has been shown that there are essentially two principal parts involved in frictional forces between two surfaces in relative motion (38,53). The first arises from the adhesive forces over the area of real contact between the two surfaces. This adhesive force is a direct result of the chemical interactions between the surfaces. These chemical interactions include covalent bonding, ionic bonding, hydrophobic-hydrophilic interactions, Van der Waals forces, and hydrogen bonding. Since the surfaces are in relative motion, these interactions play a small but significant role in the friction process.

The second, and more influential component, is that of a displacement or "plowing" term resulting from the interpenetration of asperities or protrusions on the two surfaces. The asperities interact with the opposing surface to plow into the outermost layers, thereby creating a resistance to movement of one surface relative to the other. These asperities may be the result of manufacturing or preparation of the polymer.

In addition friction between elastomers seems to be of a slightly different nature. Schallamach (54) and Roberts (55) describe a technique for looking at friction of elastomers by sliding a spherical rubber slide over a clean glass plate. They observed a buckling of the rubber, creating "waves of detachment," or Schallamach waves, which progressed from the leading edge to the back of the contact area at high speeds. A continuous dehesion occurred on one side of the wave, while the other side readhered. This frictional force was therefore not attributed to interfacial sliding; rather frictional work was associated with the energy loss of the dehesion-readhesion phenomenon. As the rubber material becomes harder the waves become smaller, and occur at high frequencies.

Two general techniques have been attempted to reduce friction in polymer systems. The first method is bonding of chemical lubricants to the surface of the polymer, the second is by surface treatment by means of radio frequency glow discharge. Two main types of chemical lubricants, hydrogels and glycosaminoglycans, show promise as friction-reducing agents. Use of a hydrogel called "Hydromer" by researchers at NIH (56) has proven to be a breakthrough in the problem of friction reduction. A nontreated catheter is defined as having a coefficient of friction (μ) of 1; the "Hydromer" showed a μ of 0.33--a significant reduction. An inherent problem with this

material is "sloughing off" of the bonded lubricant, producing possible emboli, which makes the hydrogel impractical in many clinical situations. The second chemically bonded lubricant, the glycosaminoglycans (57), shows promise as a friction-reducing agent.

Finally, the technique of RFGD applied to polymers has been extensively studied (38,58,59) and researched by means of x-ray photoelectron spectroscopy (XPS) (60,61). Radio frequency glow discharge alters the surface chemistry of the polymer, thereby changing the variables which affect friction between two polymer surfaces. This method of polymer treatment, with a flat plate geometry, has produced a 10 to 30% reduction in friction (38). Although this is not as significant as the aforementioned chemical lubricant, it does alleviate the problem of lack of surface stability.

CHAPTER 3

MATERIALS AND METHODS

3.1 Materials

3.1.1 Polyurethane 1

This catheter material was supplied by Cordis Corporation (Miami, Florida), and is given the abbreviation PU and PU_1 for the outer and inner catheters, respectively. The material is a Ducor polyurethane developed in collaboration between Dupont Chemical Company and Cordis. Infrared spectroscopy shows this material to be almost identical to the polyurethane, Pellethane. Pellethane consists of a polytetramethylene glycol soft segment, MDI (4,4' diphenylmethane diisocyanate) hard segment, and a butane diol chain extender. This polyurethane is therefore a polyether type with a combination of urea and urethane linkages. A barium sulfate filler is used to provide radiopacity.

The outer catheter (PU) is a stainless steel reinforced material with an I.D. of 0.05 in. and an O.D. of 0.10 in. The inner Ducor catheter (PU_1) has no reinforcement, an I.D. of 0.025 in. and an O.D. of 0.0425 in.

3.1.2 Polyurethane 2

This small diameter catheter material was supplied by Becton-Dickinson (Fairfield, New Jersey), and is abbreviated PU_2, for this study. This catheter was used strictly as an inner catheter for these studies. Comparison of IR spectra shows this material to have a smaller N-H stretch and a much smaller C-O stretch component when ratioed to the C-H stretch at 2800 to 3000 cm^{-1}. These facts point to a polyurethane with a higher percentage of urethane linkage and a comparatively low ether component. This is confirmed by x-ray photoelectron spectroscopy data. A bismuth oxychloride (BiOCl) compound is used as a radiopaque filler.

These catheters are not totally cylindrical, rather they are slightly eliptical due to the manufacturing process. The outer diameter of the larger part of the ellipse is 0.027 in., with the smaller at 0.024 in. The inner diameter is circular at 0.012 in.

3.1.3 Silicone Rubber

The silicone rubber catheters used in this study were donated by Cook Inc. (Bloomington, Indiana). This small diameter catheter was used only as an inner catheter for these studies. These catheters are black due to carbon (graphite) filler particles, as seen with visual microscopy. These particles are noncontiguous, which disallows electrical conductivity, as was proven by testing

with an ohmeter. No radiopaque fillers are employed in these catheters, and therefore a contrast solution must be used by the clinician to enhance visual acuity with fluoroscopic methods.

The dimensions of these catheters are: O.D. 0.033 in, ID 0.016 in.

3.1.4 Polyethylene

The polyethylene catheter used in this study is manufactured by Becton-Dickinson (Fairfield, New Jersey). It is a No. 7 French catheter with a bismuth compound used for radiopacity. The dimensions of these catheters are: O.D. 0.08 in., I.D. 0.06 in. The polyethylene catheter was used only as an outer catheter. Therefore, no treatments or testing was performed on the polyethylene catheters.

3.2 Methods

3.2.1 Preparation of Materials

Catheter sections approximately 5 cm long were prepared for x-ray photoelectron spectroscopy (XPS) and Wilhelmy plate contact angle analysis. The catheters that were friction tested were 14 cm and 30 cm for the inner and outer catheters, respectively. The first catheter material in the pair is the outer catheter and the second material is the inner.

For the in-vivo tests, outer catheters were approximately 66 cm in length; inner catheters were approximately 82 cm in length, and were treated following

the same procedures as those for XPS and contact angle analysis, explained below.

All catheters were first cleaned, as received, in a Bransonic 12 ultrasonic cleaner for 10 minutes in 95% ethanol and allowed to dry in room air for five minutes. Radio frequency glow discharge was then performed for the desired time; untreated catheters were used as controls. The materials prepared for XPS were stored in a vacuum dessicator for 24 hours prior to analysis, as a result of the excessive outgassing observed, to remove EtOH trapped in the polymer. All catheters were handled with latex rubber gloves rinsed thoroughly with distilled water. The catheters were transported and stored in sterile polystyrene petri dishes from Falcon Labware (B-D) and all fluid equilibration of the catheters was done in these same dishes.

3.2.2 Radio Frequency Glow Discharge

Radio frequency glow discharge was done in a Plasmod instrument (Tegal Corporation, Richmond, California). Cleaned samples were placed on the center portion of the sample rack located along the mid-axis of the sample chamber (Fig. 3.1). The longer catheters were wrapped around the three center cross-bars of the sample rack, maintaining a position in the center of the chamber. A schematic of the apparatus is shown in Figure 3.2. Helium (Matheson 99.99% pure) and oxygen (U.S. Welding

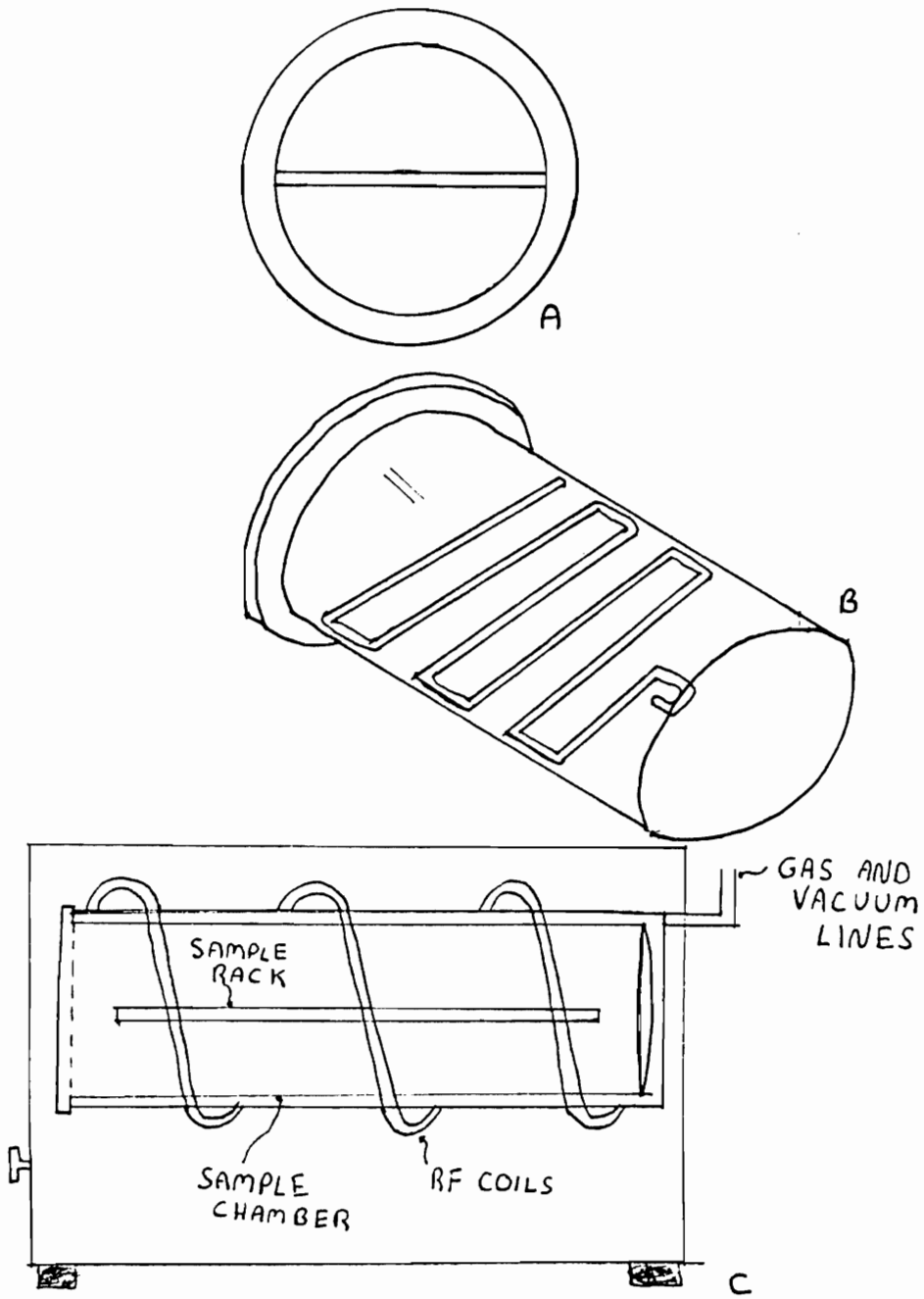

Figure 3.1 Radio frequency glow discharge apparatus. A - End-on view of sample chamber with sample rack in center. B - side view of sample chamber with sample rack. C - Side view of RFGD apparatus showing sample chamber, with sample rack, surrounded by RF coils

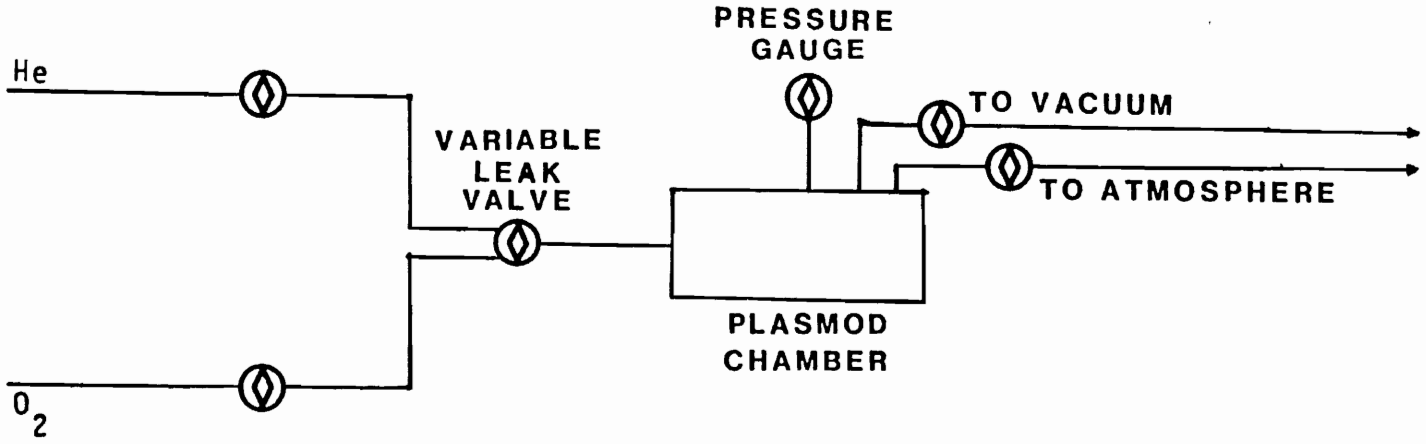

Figure 3.2 Schematic representation of the radio frequency glow discharge apparatus used in this study

Company, 99% pure) were used as the inert and reactive gases, respectively. Helium was chosen over other gases to compare and contrast with studies done by Triolo (38) in which helium was used for polymer treatment in the RFGD equipment.

The sample chamber was evacuated to 50 μHg and subsequently purged with helium (He) to atmospheric pressure. This process was repeated three consecutive times to eliminate any contaminant reactive gases present. The variable leak valve was then set to allow the chamber to equilibrate at 200 ±10 μHg. The radio frequency (RF) power was turned to approximately 35 W and the samples were treated for times of 5, 30, 120 or 300 seconds. A separate sample was utilized for each treatment time. The helium gas was then turned off and the chamber was purged with oxygen to quench any unreacted species on the surface.

The sample chamber was cleaned periodically by using high RF power for long periods of time. A positive oxygen pressure was maintained during times when the sample chamber was open to keep contaminants to a minimum.

3.2.3 X-ray Photoelectron Spectroscopy

X-ray photoelectron spectroscopy (62,63), also termed ESCA (electron spectroscopy for chemical analysis), involves exposing the specimen to a flux of monoenergetic radiation with energy $h\nu$, and observing the resultant emission of photoelectrons. The kinetic energy of these

photoelectrons is simply described by the equation,

$$h\nu = E_b + E_{KIN} + \phi_{sp}$$

in which E_b is the binding energy or ionization potential, and E_{KIN} is photoelectron kinetic energy, and ϕ_{sp} is the spectrometer work function ($\sim$4.0eV).

Once the kinetic energy of these photoelectrons is determined the resultant binding energy of the emitted photoelectrons can be computed. The kinetic energy of the photoelectrons is dependent upon the direction of emission, the radiation energy used to excite the surface of the specimen, and the chemical environment from which they came. The measurements obtained with these experiments allowed examination of the top 100 Å of the specimen.

For these experiments, a Hewlett-Packard 5950B ESCA spectrometer was utilized. This spectrometer uses Alkα monochromatized radiation at 1487 eV. The x-ray power source was run at 800 W and the analysis chamber was evacuated and samples were run at 10^{-7} to 10^{-9} torr and ambient temperatures. An electron flood gun was set at 0.5 mA and 3 eV to minimize surface charging effects. A Hewlett-Packard 9845 computer was used as an aid in the collection and processing of data.

Catheter samples were cut to fit on a copper substrate with two-sided tape to secure the catheters. The catheters were laid side by side on the substrate and covered with a gold mask containing a 3 mm x 6 mm window.

The sampling area of the spectrometer is a 1 mm x 5 mm area in the center of the window.

Wide scans of 0-1000 eV were performed to determine the elemental composition. Areas under the respective peaks were taken with the 9845 computer and atomic percent ratios were determined.

3.2.4 Contact Angle

Two methods for measuring contact angles are employed in this laboratory. First is the captive bubble technique wherein either an air or octane bubble is placed on the underside of a sample submerged in water. The dimensions of the bubble are used to calculate the contact angle, which can then be related to the surface free energy (64). This technique tends to be slow and tedious and only provides a measure of the polymer-water-air receding contact angle.

Most polymers exhibit both advancing and receding contact angles which are stable. The difference between the two angles is defined as contact angle hysteresis. This hysteresis is a function of how the sample being tested responds to the fluid in which it is immersed as well as to surface roughness and surface heterogenicity. Langmuir (65) suggested that hysteresis is a result of overturning of molecules on the surface as the liquid advances and recedes over the surface. The Wilhelmy plate

method for determining contact angle provides this information (66). This is the method used in this study.

A mechanical tester (Scott CRE/500 Mechanical Tester) raises and lowers a platform on which a beaker of 2X distilled water is placed. The rate of movement of the crosshead platform is approximately 40 mm/min. Above the platform is an electrobalance (Cahn RM-2 Ventron Corporation, Paramount, California) from which hangs a hook from which the sample to be tested is hung (Fig. 3.3). As the crosshead is raised, the sample is immersed in the water and the resultant weight differential is plotted on an Hewlett Packard X-Y recorder. As penetration of the sample continues, a straight line is produced on the recorder. This line is extrapolated to a zero depth of immersion to eliminate bouyancy effects and the mass is measured at this point. The contact angle is then determined by the equation

$$F = mg + p\gamma \cos\theta$$

or

$$\cos\theta = \frac{F-mg}{p\gamma}$$

where

m = mass of catheter (grams)

F = force measured by the balance

g = local gravitational force (979.3 dynes/gm)

p = perimeter of sample (cm)

γ = surface tension of wetting liquid; for water γ= 72.6 dynes/cm at 20°C

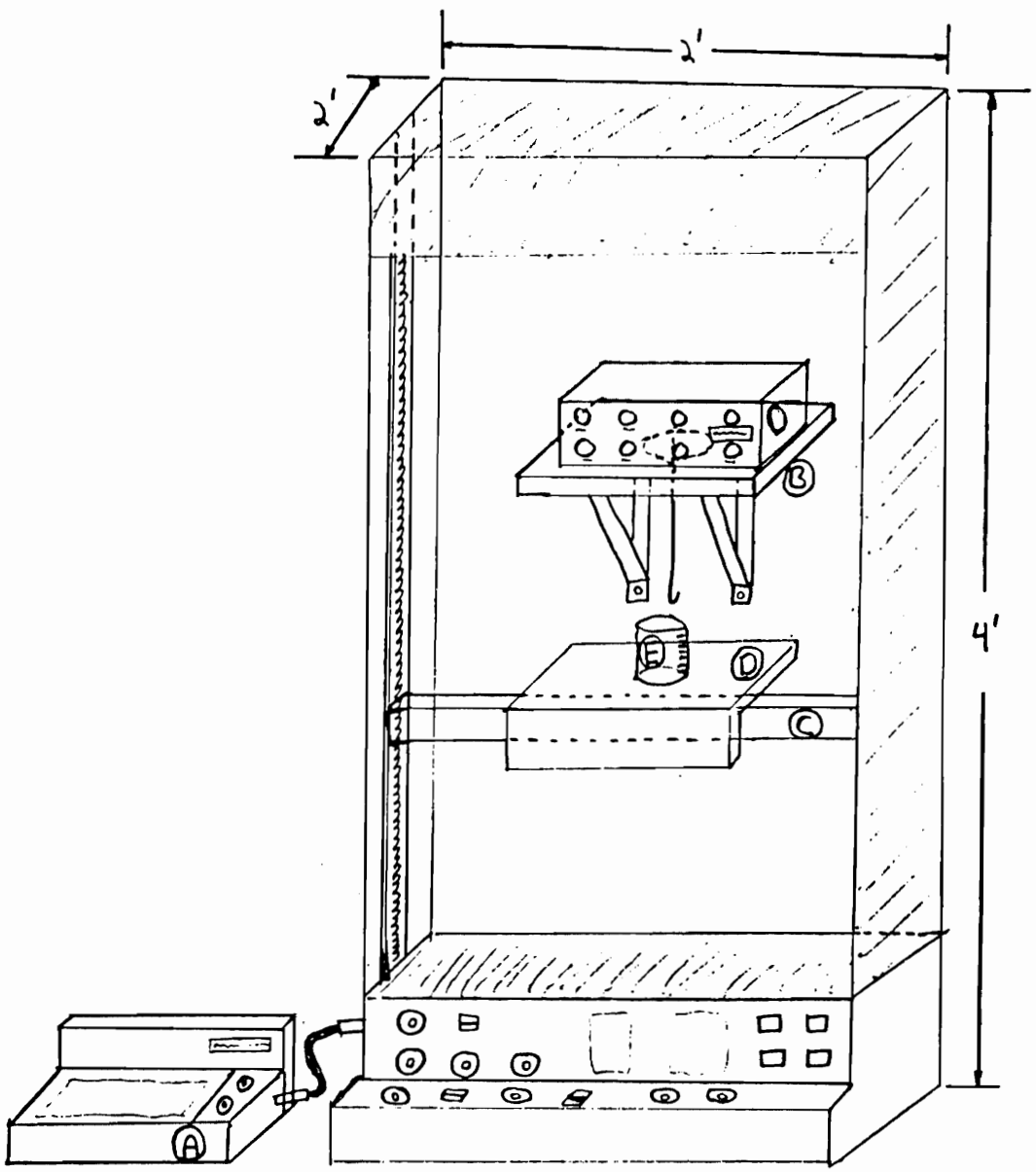

Figure 3.3 Apparatus used for determination of contact angles by the Wilhelmy plate method. A - H-P X-Y recorder. B - Electrobalance. C - Crosshead. D - Sample platform. E - Beaker for distilled water

This is shown graphically in Figure 3.4.

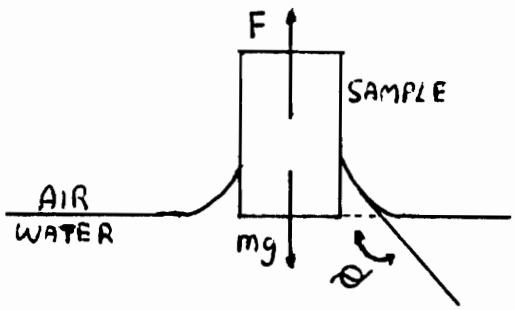

Figure 3.4 Illustration showing determination of values used for determining contact angles with the Wilhelmy Plate method

The enclosure of this apparatus is kept at a constant temperature (20°C) and constant humidity (30% RH).

The sample dimensions were first measured and the end of the catheter not to be immersed was plugged with clay (Critoseal) to eliminate capillary action. Tests were run and the catheters' dimensions were measured to determine if any swelling had occurred. For the silicone rubber catheter, a 30 AWG copper wire was inserted into the lumen to keep the otherwise flaccid material more rigid and allow for immersion of the sample.

3.2.5 Friction

Friction determinations were obtained using the apparatus shown in Figure 3.5 and a Scott-CRE/500 mechanical tester (GCA/Precision Scientific, Chicago, Illinois). A five-pound test cell (Interface Inc., Scottsdale, Arizona), is attached to the crosshead of the mechanical tester. Data is obtained on a Hewlett-Packard

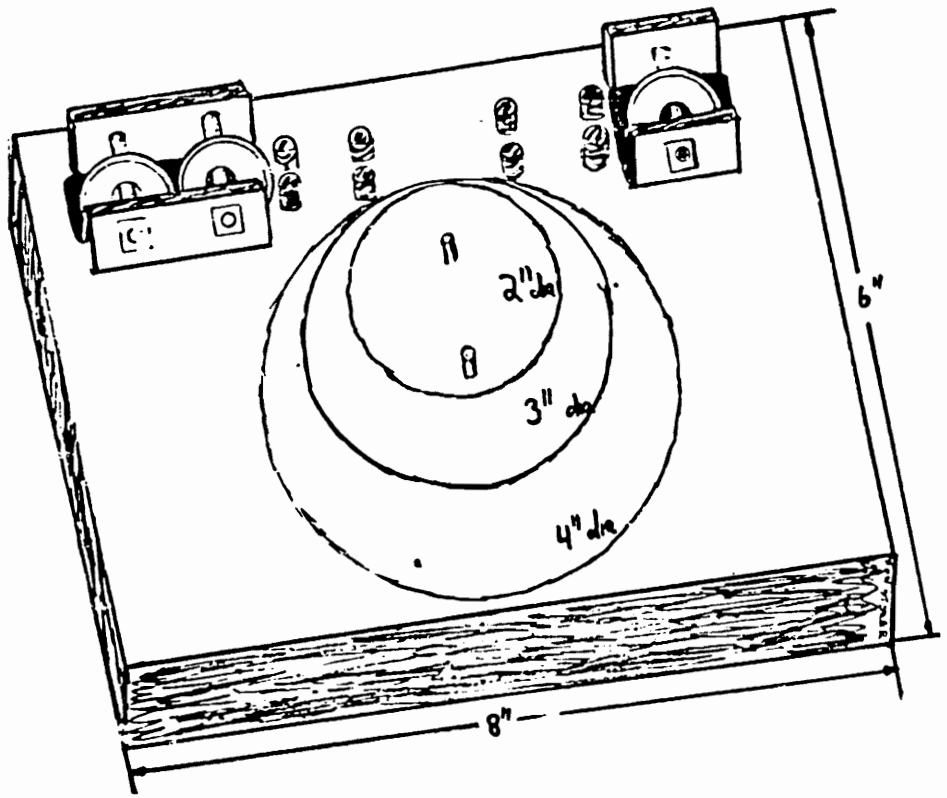

Figure 3.5 Apparatus used in the determination of friction values. An outer catheter is placed under pulleys, wrapped around the loop, and placed under the opposite pulley. The inner catheter is fed through the outer catheter and attached to a mechanical tester

X-Y recorder giving force (in pounds) as a function of crosshead distance travelled.

The dimensions of the catheter pairs determined whether 2-in diameter, 3-in diameter, or 4-in diameter test loops were used. Some pairs required that no loop be used and the catheters were laid straight across the top of the apparatus. The arrangements used are as follows:

PE-PU_1	no loop
PE-PU_2	2-in loop
PE-SR	no loop
PU-PU_1	no loop
PU-PU_2	2-in loop
PU-SR	no loop

The crosshead was lowered to a minimum point, approximately 3 cm above the top of the apparatus, and one end of the catheter was attached. On the opposite end, the inner catheter extended 13 cm beyond the end of the outer catheter. Nothing was attached to the end of the inner catheter to hinder pulling by the crosshead. The inner catheter was then pulled by the crosshead at a constant rate of 40 mm/min for 13 cm so that the same quantity of surface area was in contact throughout the test.

The wells in the apparatus were filled with either a physiologically buffered saline (PBS) at pH 7.4, PBS with 10 mg/ml albumin (Pentex bovine albumin fraction V, Miles Laboratories, Inc.) or left dry to determine the effects of different fluids in contact with the respective surfaces.

The junction between the inner and outer catheters was bathed in the wells so as to maintain a constant source of fluid between the catheter surfaces.

The testing sequence began with the control catheter being tested in the dry arrangement, followed by the 5, 30, 120, and 300 second RFGD-treated catheters also tested dry. Occasionally, the control catheter was run again to determine if any effects of continuous testing could be observed. Once the dry testing was completed, the outer catheter was primed with PBS and the wells in the test apparatus were filled with the same PBS solution. The inner catheter was initially wetted in the petri dish, in the PBS solution, inserted into the outer catheter, attached to the load cell, and tested as in the dry case. Once the inner catheter was tested, it was removed and placed in the PBS solution for four hours. During this time, the outer catheter was not maintained in solution but allowed to dry.

After four hours of hydration, the inner catheters were tested as before, the wells being filled with PBS. The inner catheters were then soaked for one hour in the albumin solution. The outer catheter was primed and the wells filled with the same albumin solution, and the friction tests were performed as before.

3.2.6 Infrared Spectroscopy

Infrared spectroscopy (IR) was performed on the two polyurethanes to aid in their chemical identification. The

spectrometer used was a Beckman Acculab I. Polyurethane 1 was dissolved in dimethyl formamide (DMF) at 3.85 mg/ml and solvent cast on a clean glass plate. A thin polymer film of PU_1 was then stripped from the glass, mounted in the spectrometer and run. Polyurethane 2 was also dissolved in DMF at 3.2 mg/ml and tested as above.

3.2.7 Mechanical Tests

Mechanical tests were performed to determine the elastic modulus of the respective catheters and were compared with literature values. The Scott-CRE/500 mechanical tester was again used with a 50-lb load cell. Only the elastic slope was obtained on the X-Y recorder.

3.2.8 In-Vivo Tests

For these tests a 20 to 25 kg male dog was used. The dog was anesthetized with a phenobarbital solution and a femoral artery cutdown was performed. The polyethylene outer catheter was advanced from the femoral artery, up the aorta to the hepatic artery, wherein it was advanced another 4 to 5 cm into the artery and left there. The 0, 5, 30, 120 and 300 second treated inner catheters (PU_1 and PU_2) were then inserted through the outer catheter, leaving enough on the distal end to tie a small knot. No fluid pretreatments were performed on the catheters used for the in-vivo study. The knot was tied to a hand-held dynamometer (FD-200, Weigh and Test Systems, Greenwich,

Connecticut), and measurements were obtained by pulling the inner catheter out at a constant rate. The maximum force values (in grams) were then recorded.

CHAPTER 4

RESULTS AND DISCUSSION

4.1 X-ray Photoelectron Spectroscopy

Carbon-oxygen ratios were obtained using Scofield theoretical cross-sections (67). Variations due to mean free path and the throughput function of the spectrometer were not taken into account in this study, since most of the spectra were obtained in the 0 to 600 eV range. In this region, the throughput and mean free path effects approximately cancel (68,69,70). Barium, used as a radiopaque filler in PU_1, is the only element with a peak located above 600 eV, at 781 and 796 eV (Ba 3d). The actual barium atomic percent is therefore smaller than that reported.

4.1.1 Polyurethane 1

Carbon-to-oxygen ratios were obtained from the XPS data as a function of treatment time (Fig. 4.1, Table 4.1). As can be seen from these results, no increase in surface oxidation was evident, which was expected in light of the relatively high oxygen content of typical polyurethanes (71). The plasma can have varied effects on the surface of the polymer and may have, therefore, altered the surface

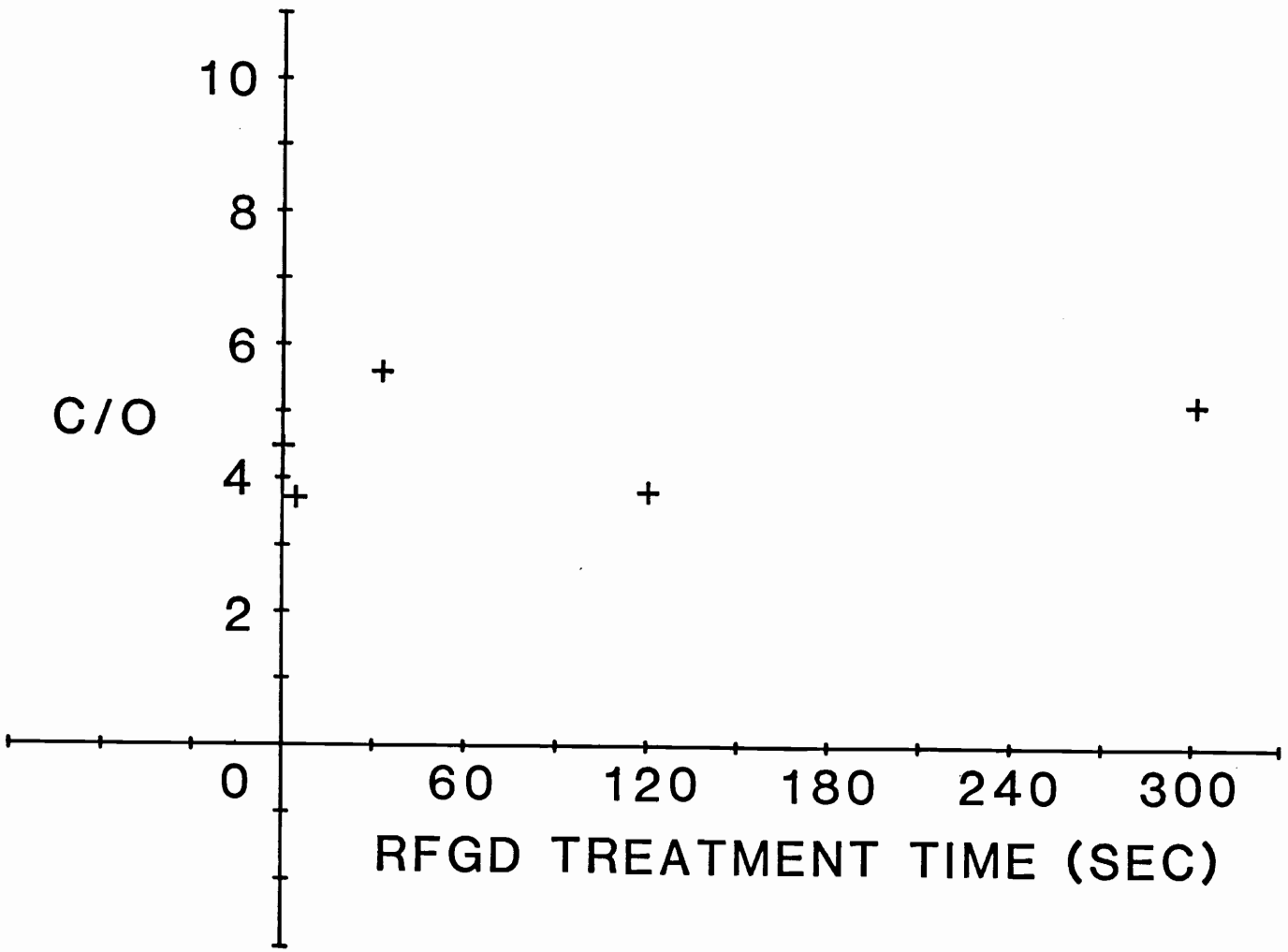

Figure 4.1 Carbon-to-oxygen ratios versus radio frequency glow discharge time for the Ducor polyurethane, PU_1

Table 4.1. X-ray photoelectron spectroscopy derived atomic percent compositions at control, 5, 30, 120 and 300 seconds for Ducor polyurethane, B-D polyurethane and silicone rubber catheters.

Atomic Percent

RFGD Treatment Time (sec)		Elements								C:O:N*/ C:O:Si
		C	O	N	Si	S	Ba	Bi	C/O	
Control	PU_1	77.9	17.6	3.0	0.6	0.7	0.2	--	4.4	26:6:1
	PU_2^1	69.8	17.4	3.0	9.5	0.3	--	0.02	4.0	20:5:1
	SR^2	40.6	30.6	0.0	28.8	--	--	--	1.3	4:3:3
5	PU_1	75.4	20.3	2.6	0.9	0.7	0.1	--	3.7	30:8:1
	PU_2^1	77.6	19.1	3.1	--	0.2	--	0.04	4.1	20:5:1
	SR^2	NA**	NA	--	--	--	--	--	--	--
30	PU_1	81.5	15.5	2.4	--	0.6	0.1	--	5.7	32:6:1
	PU_2^1	74.9	20.3	3.8	0.7	0.4	--	0.01	3.7	20:5:1
	SR^2	35.5	38.5	1.0	25.2	--	--	--	0.9	7:8:5
300	PU_1	75.2	20.2	2.7	1.0	0.7	0.2	--	3.7	30:8:1
	PU_2^1	75.7	19.2	4.1	0.4	0.3	--	0.4	3.9	20:5:1
	SR^2	24.0	46.0	0.1	29.8	--	--	--	0.5	5:9:6
	PU_1	80.6	15.6	3.7	--	--	0.1	--	5.2	31:6:1
	PU_2^1	73.2	20.8	4.2	0.4	--	--	1.48	3.5	18:5:1
	SR^2	15.0	51.4	0.4	33.1	--	--	--	0.3	3:10:7

* C:O:N = polyurethane catheters
C:O:Si = silicone rubber catheters

** No 5-second treatment of silicone rubber was examined with XPS

PU_1 = Ducor Polyurethane
PU_2^1 = B-D Polyurethane
SR^2 = Silicone Rubber (Cook)

oxygen nature, although this may not be evident due to the high oxygen content of polyurethanes such that oxidation may be obscured from the XPS analysis.

Figure 4.2 shows the effect of plasma treatment on this polyurethane. Studies in this department have shown binding energy shifts, with respect to the aliphatic carbon, of 4.0 eV and 4.6 eV for the urea, $\underset{N-\underline{C}-N}{O}$ and urethane $\underset{-O-\underline{C}-N}{O}$ functionalities, respectively. From this knowledge, it can be seen that the polyurethane used in this study has a proportionately large amount of the urea-type linkage.

Three peaks can be resolved from the C-1S spectra. One is the aliphatic carbon found primarily in the soft segment of the polyurethane. The next peak is found 1.5 eV shifted up in binding energy, most likely corresponding to ether-type functionalities. This is supported by the IR spectra. The third peak, shifted 4.0 eV, is due to the urea linkage mentioned above. These three peaks are found in a ratio of aliphatic:ether:urea of approximately 4:2:1 for the untreated catheter. As treatment time progresses, the aliphatic:ether ratio remained constant at 2:1, whereas the urea moeity progressively decreased to where, at 5 minutes of treatment time, no peak was detected. This could be evidence for degradation of the polymer surface upon long exposures to plasma treatment.

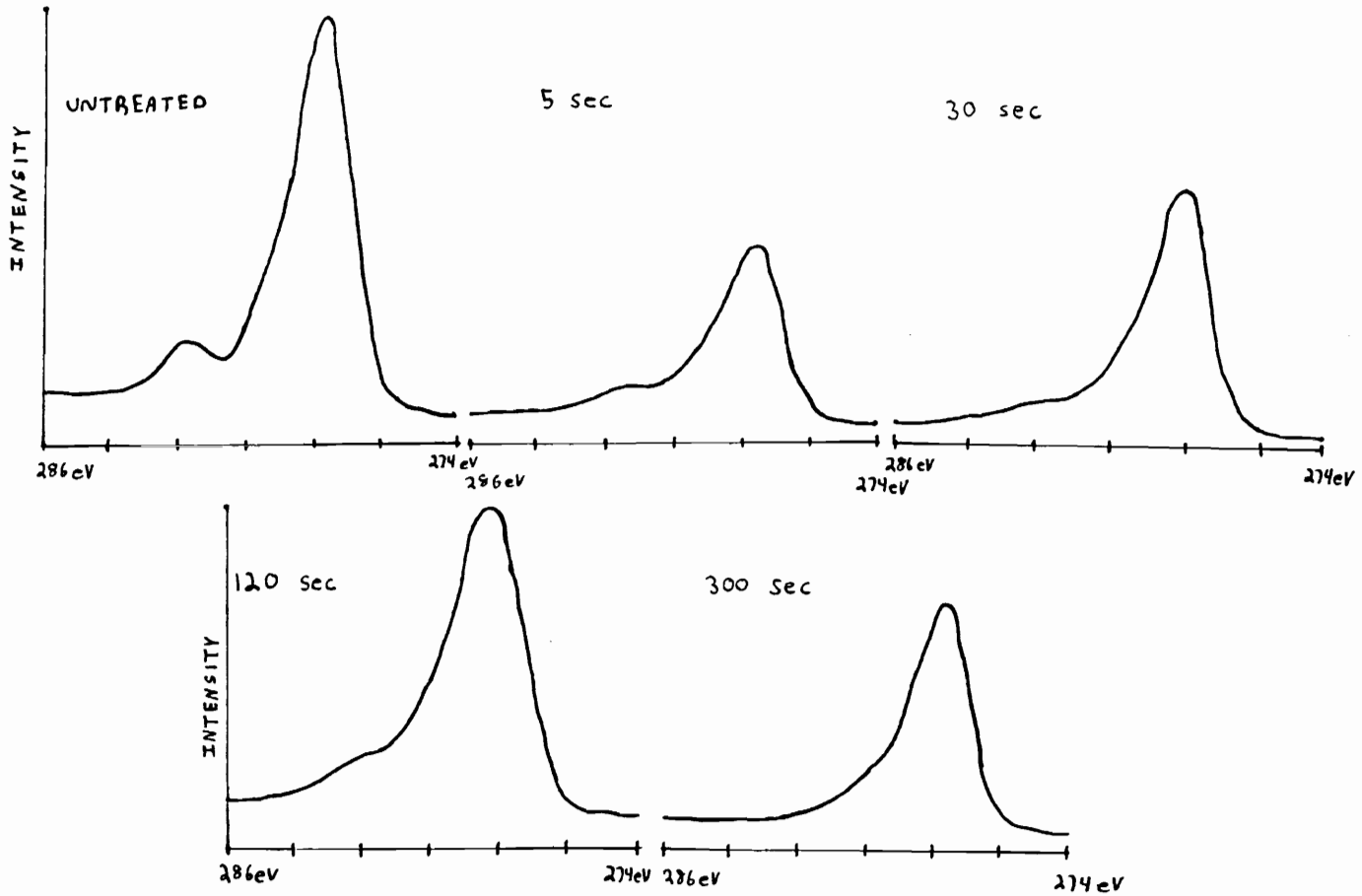

Figure 4.2 Effect of radio frequency glow discharge treatment on the urea carbon of the Ducor polyurethane shifted 4.0 eV from the main aliphatic carbon for the untreated, 5, 30, 120 and 300 second treated materials

The constant C:O:N ratio throughout the plasma treatment may be evidence for cleavage of the polymer at the urea linkage, possibly giving the urea carbon a radical or carbonium character which subsequently combines with another species to yield an amide functionality. The amide group shows a binding energy shift of 1.0 eV, and would therefore be obscured by the aliphatic carbon peak. This is supported by the fact that the full width at half maximum (FWHM), (Table 4.2) of the aliphatic peak increases from 2.0 to 2.3 eV as treatment time progresses to 5 min, and no evident oxidation occurs.

The O-1S spectra for the untreated catheter shows a large FWHM (Table 4.2), 2.75 eV, which indicates the presence of two or more oxygen species. The main peak can be resolved into two separate peaks with a ratio of 1:1 in the untreated catheter and a separation of 2.0 eV (Fig. 4.3). The higher binding energy peak corresponds to the ether oxygen and is seen to diminish with treatment time. The lower binding energy peak is most likely due to the other oxygens present on the amide and degraded urea groups. This is confirmed by the increase of the lower binding energy side of the main peak over longer plasma treatment times.

Barium sulfate ($BaSO_4$) was used as a radiopaque filler in these catheters, explaining the presence of sulfur in the spectra. Since the oxygen atomic percent

Table 4.2. Full width at half maximum and peak binding energies obtained with X-ray photoelectron spectroscopy for elemental C, O, N on PU_1 and PU_2 and C, O, Si on SR shown at RFGD treatment times of 0, 5, 30, 120 and 300 seconds.

		FWHM (eV)					BE peak (eV)***				
		RFGD Treatment Time (Sec)					RFGD Treatment Time (Sec)				
		0	5	30	120	300	0	5	30	120	300
PU_1	C	1.1	0.9	0.8	1.0	0.9	284.0	284.0	284.0	284.0	284.0
	O	1.5	1.4	1.1	1.3	1.2	531.7	531.7	531.5	531.5	531.7
	N	1.1	1.1	1.1	1.2	1.2	399.0	399.1	399.0	399.0	398.6
PU_2	C	0.8	0.9	0.9	1.0	0.9	284.0	284.0	284.0	284.0	284.0
	O	2.12	2.12	2.35	2.47	2.47	531.4	531.6	531.6	531.6	531.6
	N	1.8	2.12	2.12	2.35	2.35	399.1	399.2	399.2	399.1	399.2
SR	C	1.1	N/A**	1.3	1.3	1.9	284.0	N/A**	284.0	284.0	284.0
	O	1.4	N/A	1.9	1.9	1.8	531.7	N/A	532.0	532.2	531.9
	*Si	1.3	N/A	2.7	2.2	1.9	101.6	N/A	102.4	103.0	102.8

* Si $2p_{\frac{1}{2}}$ cross section

** No 5-sec treatment of silicone rubber was examined with XPS

*** Normalized to C-1S at 284.0eV

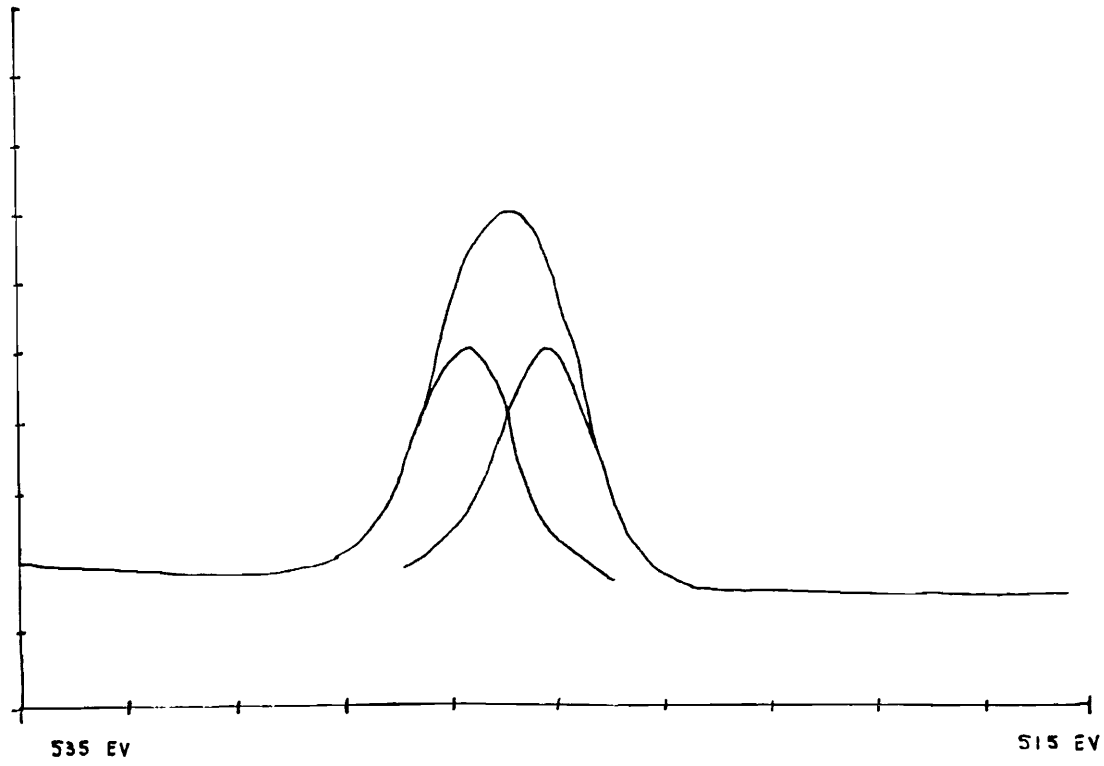

Figure 4.3 The O-1s spectra of the untreated Ducor polyurethane, PU_1, showing resolution of two peaks at 2.0 eV separation with a 1:1 ratio

remained constant throughout the plasma treatment, as well as Ba and S, it can be assumed that the oxygen present in $BaSO_4$ remained constant throughout.

The FWHM (Table 4.2) of the N-1S spectra are unchanged over treatment time, which would indicate little or no change in the nitrogen species present. The chemical shift of the urea nitrogen to an amide nitrogen is 0.4 eV, which makes separation difficult.

4.1.2 Polyurethane 2

This polyurethane, much like the previous one, shows no evidence of oxidation from the C/O ratio (Fig. 4.4, Table 4.1). This polyurethane contains an excess of urethane linkage rather than the urea of the previous catheter because of the presence of a carbon shifted 4.6 eV from the aliphatic carbon. Unlike the previous polyurethane, with this material the linkage remains intact at the same relative intensity throughout the plasma treatment. The ether functionality, at 1.2 eV shifted from the aliphatic peak, increases in height with respect to the main peak as treatment time increases. This may be due to an oxidation of the polymer in the aliphatic chain of the soft segment producing the ether moeity.

A disparity occurs with the increasing ether functionality in that the atomic percent oxygen remains constant throughout the treatment time. A possible

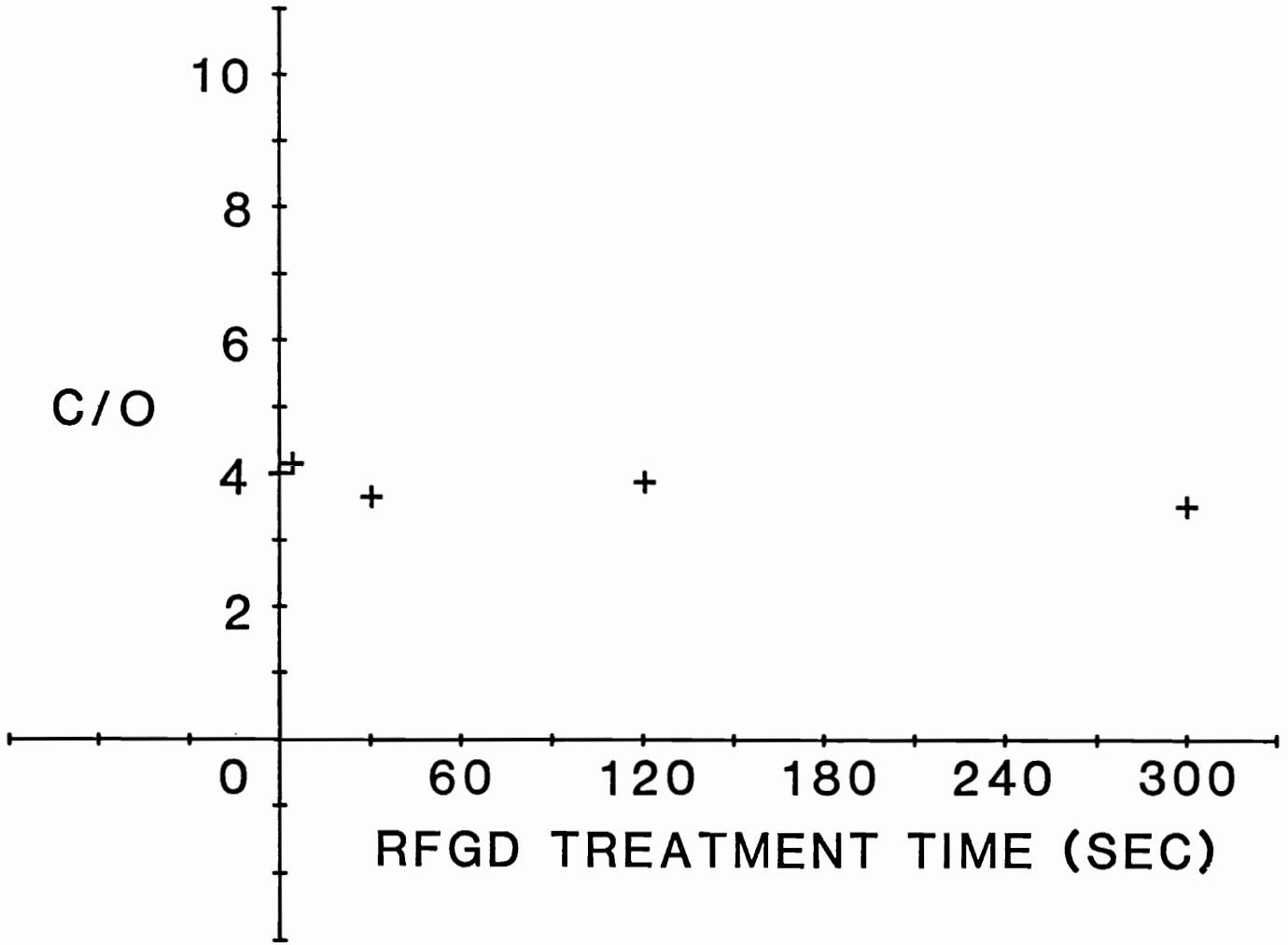

Figure 4.4 Carbon-to-oxygen ratios vs. radio-frequency glow discharge times for the Becton-Dickinson polyurethane, PU_2

explanation is that the FWHM of the very symmetrical O-1S peak increases 2.1 to 2.5 eV over time as the ether carbon increases (Table 4.2). Here a concommitant increase is seen in both the carbon and oxygen quantity, as well as nitrogen, producing a constant C:O:N ratio (Table 4.1).

The N-1S spectra shows an increasing FWHM from 1.8 to 2.35 eV over the 5-min treatment time (Table 4.2). This is obvious evidence for a change in the nitrogen species present. Although this is contradictory to the C-1S spectrum, which shows no change in the relative height of the urethane carbon, it may be that the nitrogen shows more urea-type character, as supported by the increasing FWHM of the urethane carbon peak found 4.6 eV shifted upfield from the main aliphatic peak (Table 4.2).

The radiopaque filler used for this catheter is bismuth oxychloride (BiOCl). Etching and removal of a surface layer of polymer by the RFGD process may have exposed more filler at the surface. The relatively small amount of bismuth present on the surface of the untreated catheter increases dramatically over treatment time, some 700 times. Since no chlorine was observed in any of the spectra, it is possible that the chlorine was replaced by an oxygen- containing group. This could have possibly affected the Bi in such a way as to expose it more on the surface of the polymer. This new bismuth filler would then aid in the increase of the O-1S FWHM seen.

4.1.3 Silicone Rubber

The carbon:oxygen:silicon ratio of the untreated silicone rubber catheter was 10:8:7. The backbone for pure polydimethylsiloxane (PDMSO) is $\left(\begin{smallmatrix} CH_3 \\ | \\ Si\text{-}O \\ | \\ CH_3 \end{smallmatrix}\right)_n$, which gives a C:O:Si of 2:1:1. Therefore a discrepancy exists suggesting that the catheter material is not a pure PDMSO. Since no graphite particles seem to be present on the surface (Sec. 3.1.3) it may be that a silica filler was used in these catheters. The presence of $SiO_2(O\text{-}Si\text{-}O)_n$, on the surface with the PDMSO and a PDMSO/SiO_2 ratio of 2:1 would give a C:O:Si of 4:4:3. The table below shows different PDMSO/SiO_2 ratios and the corresponding C:O:Si ratios.

PDMSO/SiO_2	C:O:Si
1:1	2:3:2
2:1	4:4:3
1:2	2:5:3
3:1	6:5:4
1:3	2:7:4
3:2	6:7:5
2:3	4:8:5
1:4	2:9:5
4:1	8:6:5

When comparing this table to Table 4.1 it can be seen that the untreated catheter shows a C:O:Si of 4:3:3, which corresponds to a PDMSO/SiO_2 of approximately 2:1. The 30 second treated catheter shows a C:O:Si of 7:8:5 which is close to a 1:1 PDMSO/SiO_2 ratio. Continuing on, the 120 second treated catheter with a C:O:Si of 5:9:6 corresponds to a PDMSO/SiO_2 of approximately 1:3, and, finally, the 300 second treated catheter shows a C:O:Si of 3:10:7 which closely resembles a PDMSO/SiO_2 of 1:4. From this data it can be deduced that there exists on the surface of these catheters an SiO_2 filler which upon RFGD treatment becomes more prevalent, i.e., becomes more exposed on the surface. Fig. 4.5 and Table 4.1 show marked decreases in the atomic percent obtained for carbon and an increase in oxygen and silicon content. This is support for the increased expression of SiO_2 on the surface with increasing RFGD treatment time.

Figure 4.6 and Table 4.2 show that as treatment time progresses, the FWHM for Si2p increases, peaks and comes down again. At the same time the peak binding energy shifts upfield. This is again strong evidence for the presence of a silica filler, or possibly a mold release agent, on the surface of these catheters. The SiO_2 becomes more prevalent as RFGD treatment time increases most likely because surface reactions occur in which methyl groups from PDMSO are released by the energetic plasma and replaced with branching SiO_2 units.

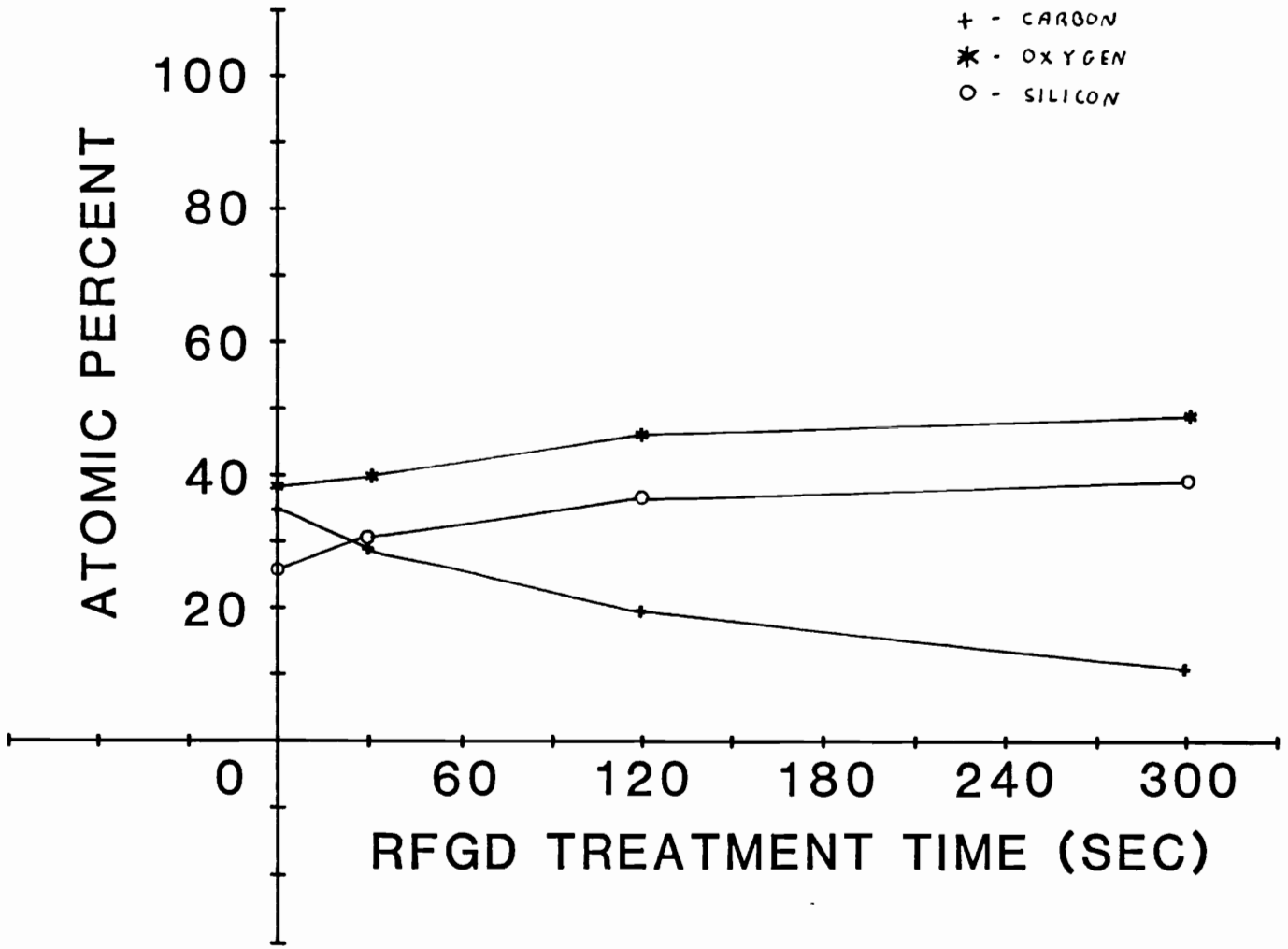

Figure 4.5 Atomic percent of C, O, Si as a function of radio-frequency glow discharge treatment time for the silicone rubber catheter

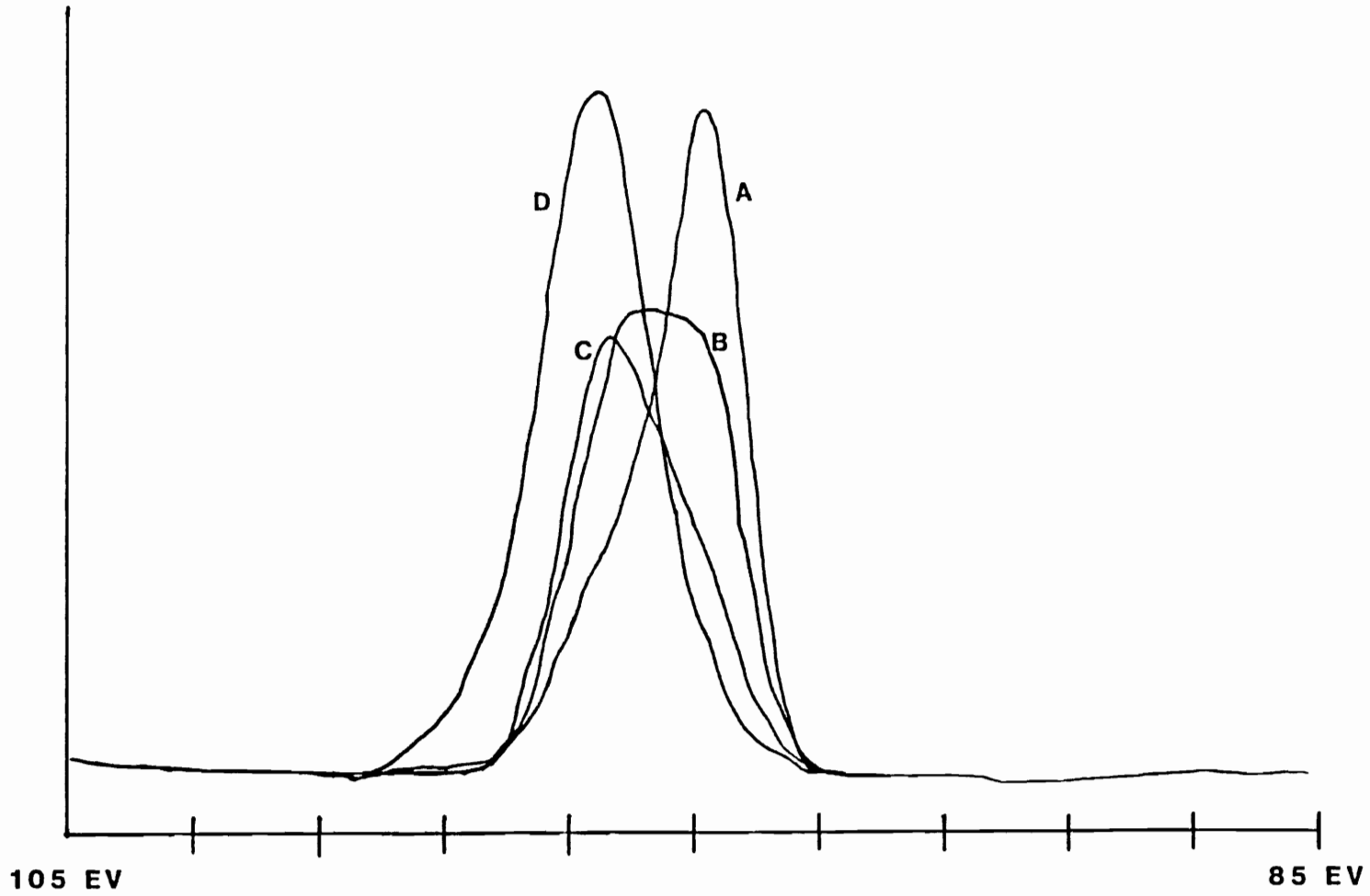

Figure 4.6 The Si-2p spectra versus radio frequency glow discharge treatment time for the silicone rubber catheter. A - Untreated. B - 30 second treated. C - 120 second treated. D - 300 second treated

The O-1s peak shows a significant increase in the FWHM as the treatment time progresses from 0 to 30 seconds (Table 4.2). This implies a change in the type of oxygen environment present for the SiO_2 versus PDMSO oxygen after exposure to the plasma. The decreasing carbon-oxygen ratio (Table 4.1), is again evidence for replacement of methyl side group by oxygen containing groups.

SiO_2 is a likely surface by-product of the methyl cleavage of PDMSO, which may further explain the decreasing carbon-oxygen ratio. Feneberg et al. (72) have also suggested the existence of SiO_2 on the surface of PDMSO and other organopolysiloxane elastomers after ion bombardment.

Triolo (38), using PDMSO spun cast on a glass microscope slide, also found large increases in oxygen percent after 300 second RFGD treatments. He concluded that with long treatment times almost all of the silicon and carbon was bound to two oxygens. The work done here does not support this conclusion, since a C:O:Si of 3:10:7 for the 300 second treated catheters could not possibly consist of two oxygens per carbon and silicon. This is again evidence for the existence of an SiO_2 filler on the surface of the catheter. The discrepancy between this work and that done previously is that Triolo used pure PDMSO, and the materials used in these experiments were fabricated catheters with impurities and fillers present in the PDMSO.

The quantity of nitrogen present on the surface was unchanged over treatment time, remaining at approximately one half of one percent, with no nitrogen present on the untreated catheters. The nitrogen present on the treated catheters was most likely due to atmospheric nitrogen being incorporated during or after RFGD treatment by reactive species on the surface.

4.2 Contact Angle

Contact angle is a much more sensitive surface analysis method than standard XPS, in that it is a measure of the outermost 5 to 10 Å of a material. Table 4.3 gives the results obtained for contact angles of all three inner catheter materials. Three to five tests were performed for each material at the previously specified treatment times.

4.2.1 Polyurethane 1

Table 4.3 and Figures 4.7 and 4.8 show the data for this polyurethane. A 23% decrease is found for the advancing water angle, and a 32% reduction is obtained for the receding angle from the untreated to the 5-second-treated material. The remaining points stay within the standard deviation value of the 5-second point. Although the XPS analysis showed no sign of surface oxidation, the contact angle points to a definite increase in the polar nature of the surface upon initial exposure to RFGD. It is possible that the polyurethane is very resistant to

Table 4.3 Advancing and receding water contact angles for PU_1, PU_2 and SR at radio frequency glow discharge treatment times of 0, 5, 30, 120 and 300 seconds.

Water Contact Angle

Contact Angle (Degrees)		Radio Frequency Glow Discharge Treatment Time				
		Control	5 sec	30 sec	120 sec	300 sec
PU_1	θ_{adv}	83 ± 3	66 ± 3	64 ± 5	64 ± 7	63 ± 10
	θ_{rec}	38 ± 2	24 ± 5	27 ± 3	24 ± 4	27 ± 2
PU_2	θ_{adv}	82 ± 2	59 ± 4	60 ± 8	64 ± 1	64 ± 1
	θ_{rec}	48 ± 5	29 ± 1	25 ± 2	27 ± 1	37 ± 2
SR	θ_{adv}	125 ± 4	107 ± 8	99 ± 7	97 ± 2	68 ± 20
	θ_{rec}	82 ± 1	71 ± 3	71 ± 5	65 ± 3	39 ± 18

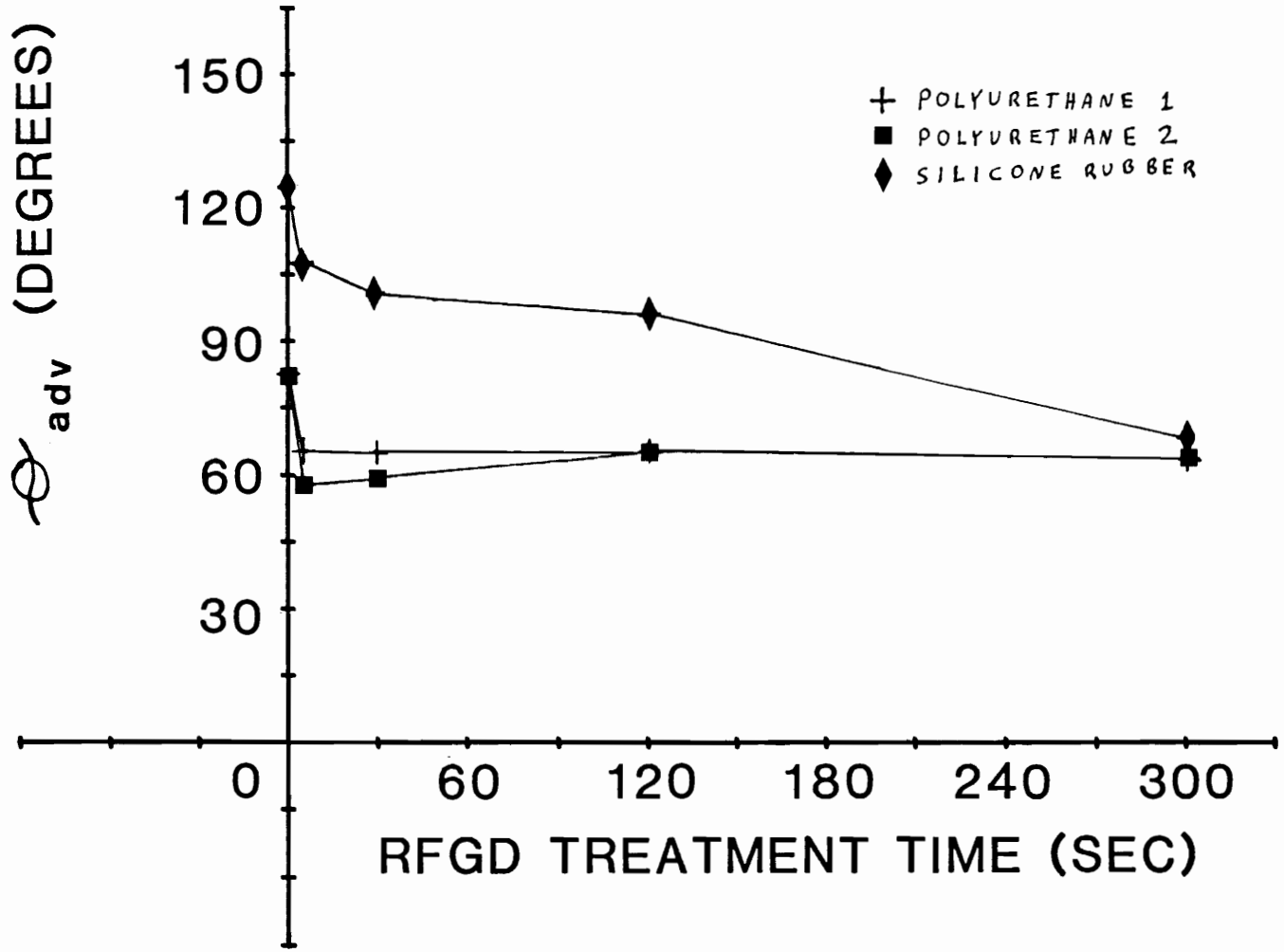

Figure 4.7 Advancing water contact angle as a function of radio-frequency glow discharge treatment time for the treated inner catheters; polyurethane 1, polyurethane 2 and silicone rubber

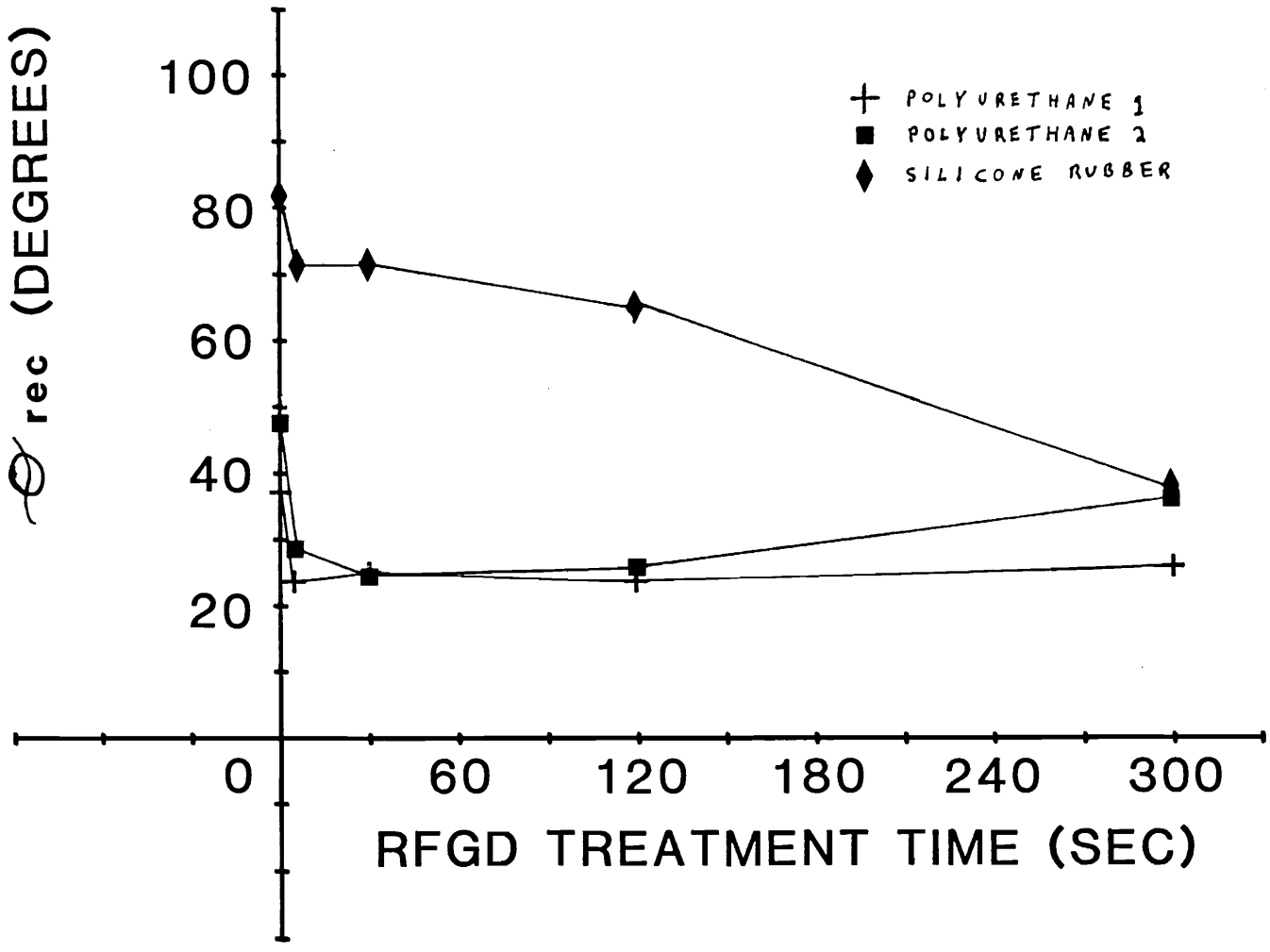

Figure 4.8 Receding water contact angle as a function of radio-frequency glow discharge treatment time for the treated inner catheters; polyurethane 1, polyurethane 2 and silicone rubber

oxidation and only the outermost molecular layers are involved with any surface chemistry. This again may be evidence for the photodegradation of the polymer, as expressed in the XPS data.

Pellethane (Sec. 3.1), a pure polyurethane of which these catheters are similar, shows a dry (nonhydrated) advancing water angle of 87 ± 1 degrees, and a receding angle of 51 ± 1 degrees. These values are close to those obtained for polyurethane 1 (Table 4.3).

4.2.2 Polyurethane 2

This catheter shows much the same behavior (Table 4.3) as the previous polyurethane. The advancing and receding angles, as a function of RFGD treatment, are shown in Figures 4.7 and 4.8, respectively. The advancing angle decreases 24% over the first 5 seconds of treatment, as with PU_1. A larger decrease is obtained, 43%, for the receding angle. The reason for this is unknown. Again, as with PU_1, the contact angle reached a plateau value after 5 seconds of RFGD treatment in both advancing and receding angles.

4.2.3 Silicone Rubber

As seen from Table 4.3 and Figures 4.7 and 4.8, the contact angle displays a rapid decrease from the zero to 5-second treatment, a levelling off to the 120-second point, and an even more rapid drop to the 300-second point.

This may be evidence to support the hypothesis that silicon oxidizes preferentially to carbon until longer treatment time has transpired, as noted with the XPS data.

A small study was performed to assess the effects of RFGD on the surface roughness of the silicone rubber catheters. With visual microscopy, 400X, no detectable difference was observed in the surface roughness of the untreated, EtOH-cleaned, and 5-minute-RFGD-treated catheters. All materials showed a smooth surface at approximately a 2.5μ level.

Other contact angle data with a pure PDMSO (73) shows much lower values for both advancing (89° ± 3.2°) and receding 55° ± 1°) angles than those obtained for the untreated catheter material used in this study.

4.2.4 Conclusions

No correlation was established between the atomic percent of oxygen, as determined by XPS, and the advancing or receding contact angles for any of the catheter materials studied.

Because the polyurethane catheters are already oxygen rich (71) any further oxidation would result in a small percentage oxygen increase not likely to be detected with XPS. If polystyrene, polyethylene or any other hydrocarbon polymer were used, a change in oxidation, as measured by XPS, would correlate well with the contact angle (37). It may therefore be concluded from the contact

angle analysis that oxidation of the surface did occur, even though it was undetected with XPS analysis.

With the silicone rubber catheters a definite correlation can be observed between the carbon-oxygen ratio and the advancing or receding contact angle. From Table 4.1 and Table 4.3 it can be seen that both the carbon-oxygen ratio and contact angles, advancing and receding, decrease with increasing treatment time.

4.3 Friction

4.3.1 Discussion

Triolo (37) described five different types of behavior for polymer sliding friction with a flat-plate geometry.

Type "A" (Fig.4.9a). Many high-amplitude, low-frequency spikes are observed. The peaks are sharp with steep slopes. This type of behavior seems to be a stick-slip nature as a result of repeatedly overcoming the adhesive or mechanical bonding of the two surfaces. The rapid rise and descent is indicative of a sticking followed by a jump to the next point of adherence.

Type "B" (Fig. 4.9b). This behavior showed high-amplitude, low-frequency peaks separated by sections of lower force. Rise time is greater for the peaks than in "A." Peaks are sharp and fall rapidly. This type of behavior seems to be indicative of an elastomeric response,

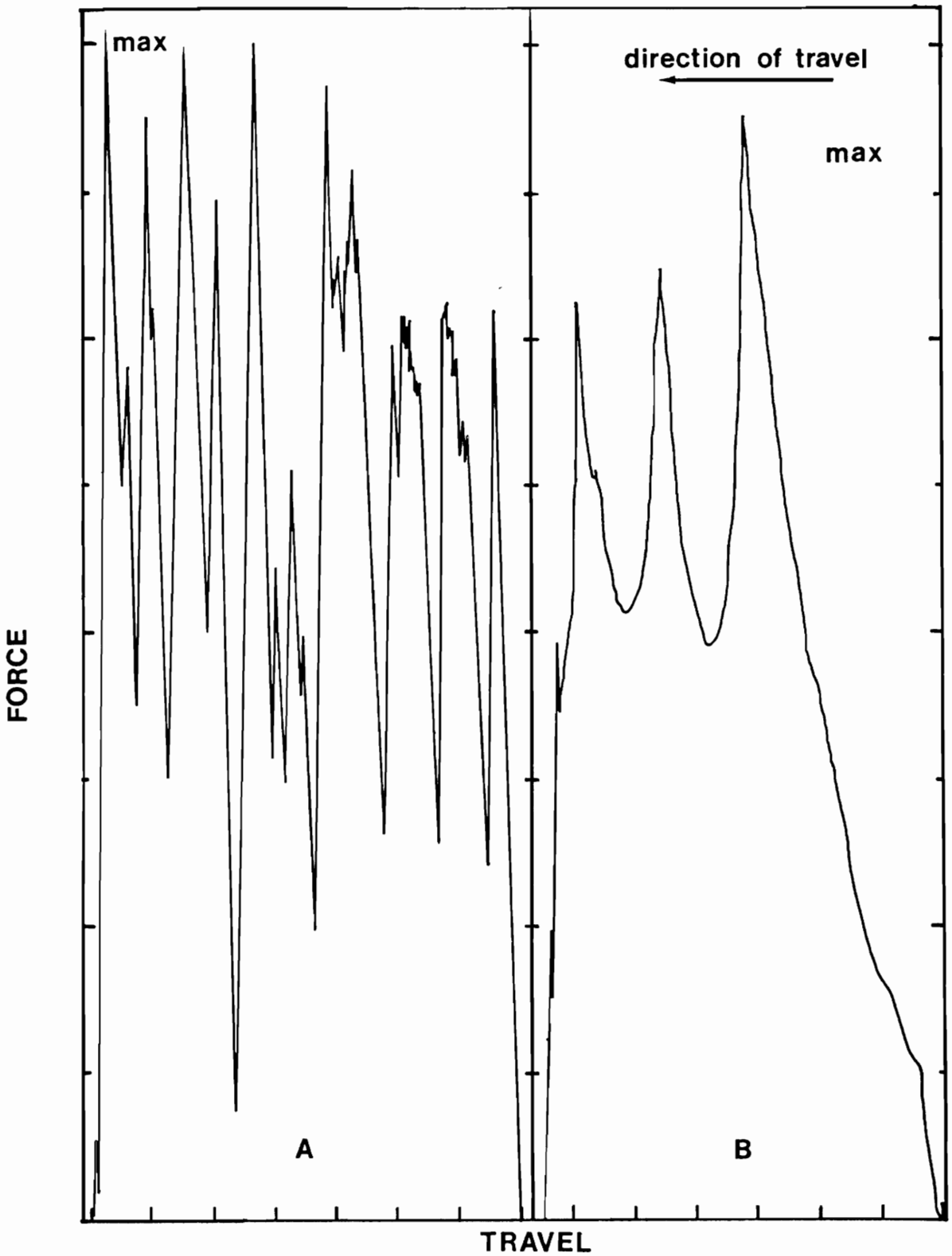

Figure 4.9a,b Representative graphs produced by friction types "A" and "B." (See text for description.)

where the slow rise time is allowing a greater stretch of the material, i.e. a greater energy storage. Once the elastomer is stretched, the stress overcomes the adhesive or mechanical bonds, causing the material to jump. This behavior is simply the elastomeric counterpart of type "A."

Type "C" (Fig. 4.9c). Low-amplitude, high-frequency spikes predominate, the opposite of type "B" friction. With type "C," the material is rigid and does not allow the storage of energy to produce the high amplitude peaks. It may also be that the polymers involved do not display as great an interfacial force to resist the pulling force. Type "C" is again a stick-slip friction, which is of lower degree than type "A" or type "B," to produce the low-amplitude, high-frequency peaks.

Type "D" (Fig. 4.9d). A relatively smooth curve is obtained with a small spike at the beginning of the force versus distance curve. The remainder of the curve displays a relatively constant value. This is typical of most materials in that a larger force is required to initiate movement (static friction) than is required to maintain movement (dynamic friction). Not much energy is stored in the surface and adhesive or mechanical bonds fall readily. The force value in this case is largely dependent on the weight of the material.

Type "E" (Fig. 4.9e). According to Triolo (37), type "E" behavior is a combination of type "A" and type "D" behaviors. A net storage of energy occurred in the polymer

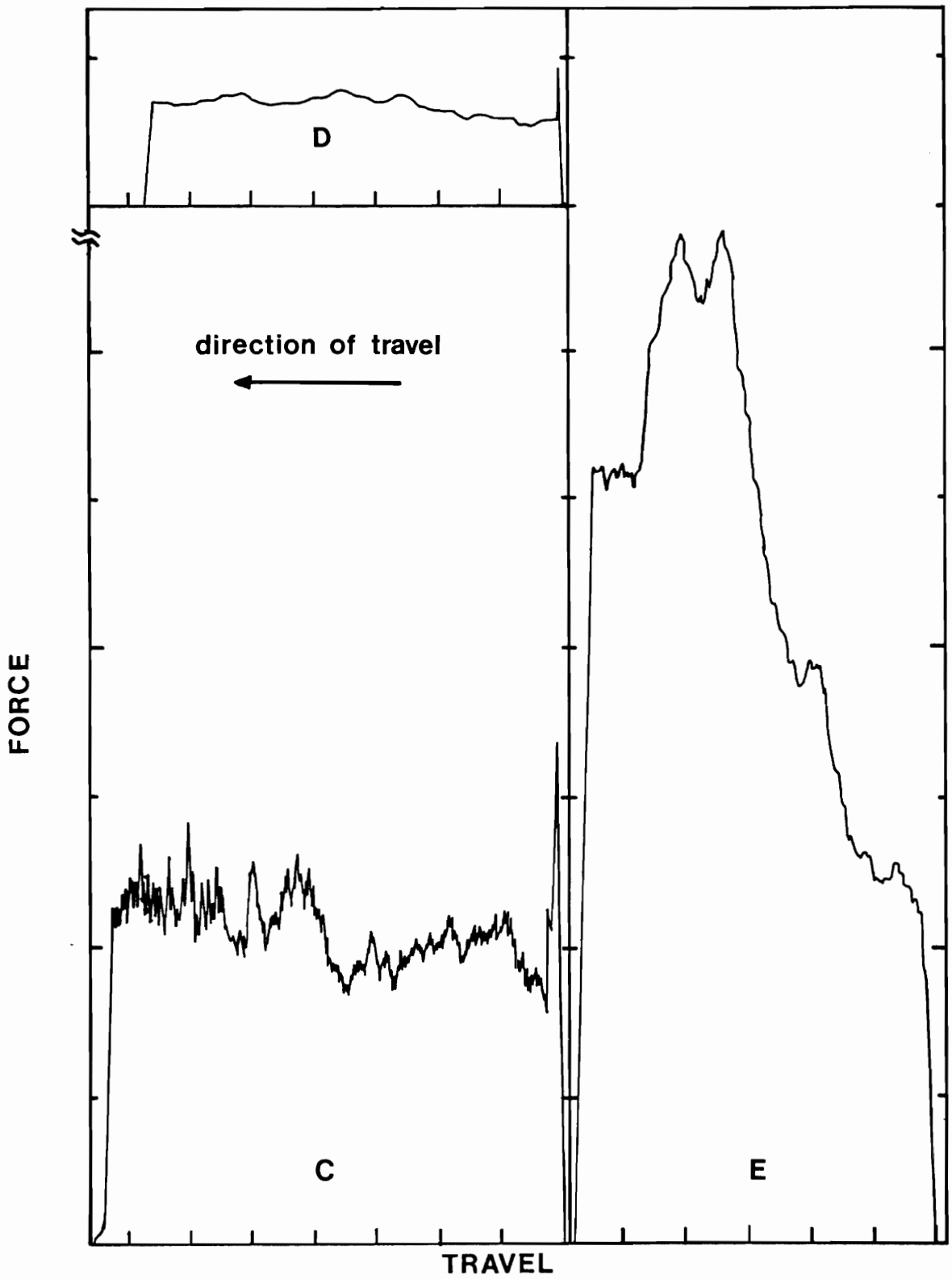

Figure 4.9c,d,e Representative graphs produced by friction types "C," "D," and "E." (See text for description.)

surfaces as a result of the pulling force being applied. This resulted in an increased force required to maintain a relative motion between the two surfaces. For Triolo's experiments, no abrupt failure of the interfacial forces occurred during the sliding period. He postulates that perhaps a plateau value would have eventually been obtained where the net energy input was balanced by the elastic recovery of the system.

For the experiments in this study, the predominant behavior was those of types "B," "C," and "D." This will be discussed as each of the results is presented. The fluids used are represented as letters. "A" refers to the dry test; "B" is an initial wetting with PBS, with the wells filled again with PBS; and finally "D" is a one-hour soak in a 10 mg/ml albumin solution with the wells being filled with the same albumin solution.

The data were obtained by reading off five points from the X-Y tracings, at intervals of approximately 3 cm of catheter pulled. These points were averaged and used as the final data value for each respective test. This procedure was chosen because the curves produced by these experiments reached a plateau level after the motion of the inner catheter began. A maximum friction value for each test and the maximum values were averaged over three tests (Table 4.4).

Table 4.4 Friction values for the catheter pairs PE-PU_1, PE-PU_2, PE-SR, PU-PU_1, PU-PU_2, and PU-SR for radio frequency glow discharge treatment times of 0, 5, 30, 120 and 300 seconds. The average force, standard deviation and average maximum value for three tests per catheter pair is given. The friction values for each catheter pair are given for four different solutions.

		Radio Frequency Glow Discharge Treatment Time									
		Control		5 sec		30 sec		120 sec		300 sec	
Catheter	Sol'n*	Force (S.D.) (gm)	$\overline{Max}$	Force (S.D.) (gm)	$\overline{Max}$	Force (S.D.) (gm)	$\overline{Max}$	Force (S.D.) (gm)	$\overline{Max}$	Force (S.D.) (gm)	$\overline{Max}$
PE-PU_1	A	36.9 ± (6.3)	39.6	37.6 ± (2.8)	42.0	39.7 ± (1.9)	46.8	37.3 ± (2.0)	44.5	45.2 ± (8.5)	49.9
	B	30.5 ± (3.3)	33.4	33.2 ± (2.3)	38.5	33.1 ± (3.3)	37.7	31.9 ± (4.8)	38.6	33.3 ± (4.1)	37.2
	C	21.1 ± (2.6)	30.4	29.2 ± (2.3)	35.5	30.4 ± (6.1)	36.6	27.2 ± (2.6)	32.2	29.8 ± (3.0)	34.1
	D	33.5 ± (6.7)	37.8	40.6 ± (2.6)	48.2	46.3 ± (7.1)	53.5	40.3 ± (6.4)	47.9	40.9 ± (9.2)	49.3
PE-PU_2	A	9.4 ± (2.9)	11.7	11.5 ± (4.1)	16.6	14.6 ± (7.9)	21.6	13.0 ± (2.8)	18.1	13.2 ± (4.2)	23.0
	B	6.1 ± (2.7)	8.5	6.1 ± (1.5)	8.9	8.8 ± (0.7)	11.4	5.5 ± (1.8)	7.4	8.4 ± (4.5)	11.8
	C	5.0 ± (1.7)	6.8	4.5 ± (2.6)	7.4	5.6 ± (2.5)	8.0	5.4 ± (1.4)	8.0	4.4 ± (1.1)	8.0
	D	13.1 ± (5.9)	21.3	18.0 ± (9.1)	29.3	18.8 ± (8.8)	28.2	18.7 ± (9.7)	28.6	15.4 ± (3.4)	29.5
PE-SR	A	5.0 ± (1.3)	8.7	7.3 ± (1.6)	12.5	9.3 ± (0.5)	13.0	6.0 ± (1.1)	8.1	4.0 ± (1.1)	6.8
	B	4.0 ± (1.0)	8.7	5.0 ± (0.3)	8.2	3.8 ± (0.6)	5.7	4.6 ± (1.4)	6.7	3.5 ± (0.9)	5.1
	C	3.7 ± (0.9)	8.4	5.5 ± (0.7)	6.8	3.9 ± (0.6)	5.7	3.4 ± (0.6)	5.0	2.9 ± (0.6)	4.4
	D	2.6 ± (0.4)	4.3	3.0 ± (0.6)	5.3	3.3 ± (0.8)	6.5	3.1 ± (0.5)	4.9	2.9 ± (0.2)	4.8
PU-PU_1	A	136.7 ± (29.2)	169.2	151.4 ± (12.1)	177.3	123.2 ± (22.3)	143.3	206.1 ± (5.0)	249.1	208.7 ± (8.0)	248.2
	B	114.2 ± (10.7)	140.6	95.3 ± (13.7)	114.2	90.3 ± (8.9)	119.7	119.8 ± (9.6)	153.1	151.1 ± (34.6)	193.2
	C	113.9 ± (5.6)	142.5	94.5 ± (20.0)	108.5	92.3 ± (13.6)	112.3	112.7 ± (7.2)	141.0	127.2 ± (10.3)	165.9
	D	143.7 ± (22.3)	183.3	131.8 ± (27.3)	162.2	113.3 ± (14.9)	138.1	145.5 ± (4.7)	186.4	162.2 ± (15.2)	215.1
PU-SR	A	122.0 ± (28.9)	174.5	100.2 ± (33.4)	162.5	152.3 ± (12.1)	214.7	106.8 ± (21.9)	176.1	109.9 ± (22.9)	184.5
	B	85.0 ± (36.1)	155.0	69.0 ± (46.6)	141.4	56.2 ± (17.7)	115.7	52.6 ± (9.5)	93.0	54.0 ± (11.4)	128.5
	C	63.6 ± (6.0)	134.6	52.5 ± (6.2)	109.6	40.6 ± (15.1)	83.5	39.2 ± (9.3)	88.5	31.8 ± (4.8)	60.1
	D	91.5 ± (23.8)	143.6	73.9 ± (3.0)	122.5	91.8 ± (13.8)	149.7	84.7 ± (13.5)	139.1	100.3 ± (21.3)	155.0
PU-SR	A	16.6 ± (5.2)	22.3	12.1 ± (1.4)	15.6	18.3 ± (1.6)	24.7	14.0 ± (0.8)	18.1	4.4 ± (1.0)	8.2
	B	2.8 ± (0.7)	3.8	5.0 ± (0.1)	7.6	7.6 ± (5.1)	11.1	3.3 ± (0.1)	5.0	3.7 ± (0.8)	5.5
	C	3.2 ± (0.3)	4.2	4.9 ± (0.1)	7.4	2.9 ± (0.5)	4.4	3.0 ± (0.6)	4.4	2.4 ± (0.3)	3.2
	D	3.3 ± (0.7)	4.2	5.3 ± (0.7)	6.7	4.2 ± (0.5)	4.9	3.8 ± (0.9)	4.6	3.4 ± (0.2)	3.9

* A = Dry
B = Wetted
C = Hydrated 4 Hrs
D = 10 mg/ml Albumin

PE = B-D Polyethylene
PU_1 = Ducor Polyurethane
PU_2 = B-D Polyurethane
SR^2 = Cook silicone rubber

4.3.2 Polyethylene-Polyurethane 1

Table 4.4 and Figures 4.10 and 4.11 show the results of friction tests with this catheter pair, polyethylene being the outer and PU_1 being the inner catheter. Figure 4.10 shows no affect of RFGD treatment time on friction. A relatively constant friction value is obtained at all treatment times for each of the various fluids.

Figure 4.11 shows friction as a function of the fluids utilized for this study for each of the RFGD treatment times. For each of the treatment times, the friction decreased from the dry system (A) to the wetted system (B). The friction then decreased again from the wetted to the hydrated system (C). Upon pretreatment of the polyurethane catheter in the albumin solution (D), the friction increased. The values obtained for the albumin system were higher than those of the dry system for the 5-, 30-, and 120-second treatments, and remained slightly lower for the control and 300-second treatment.

The catheter pair exhibited a combination of type "C" and "D" behaviors. The tracings displayed very small-amplitude, high-frequency peaks intermixed with periods of relatively smooth, constant values. This behavior would be indicative of a relatively rigid catheter, with a small amount of stick-slip behavior as a result of either small interfacial forces or a weak elastomeric component.

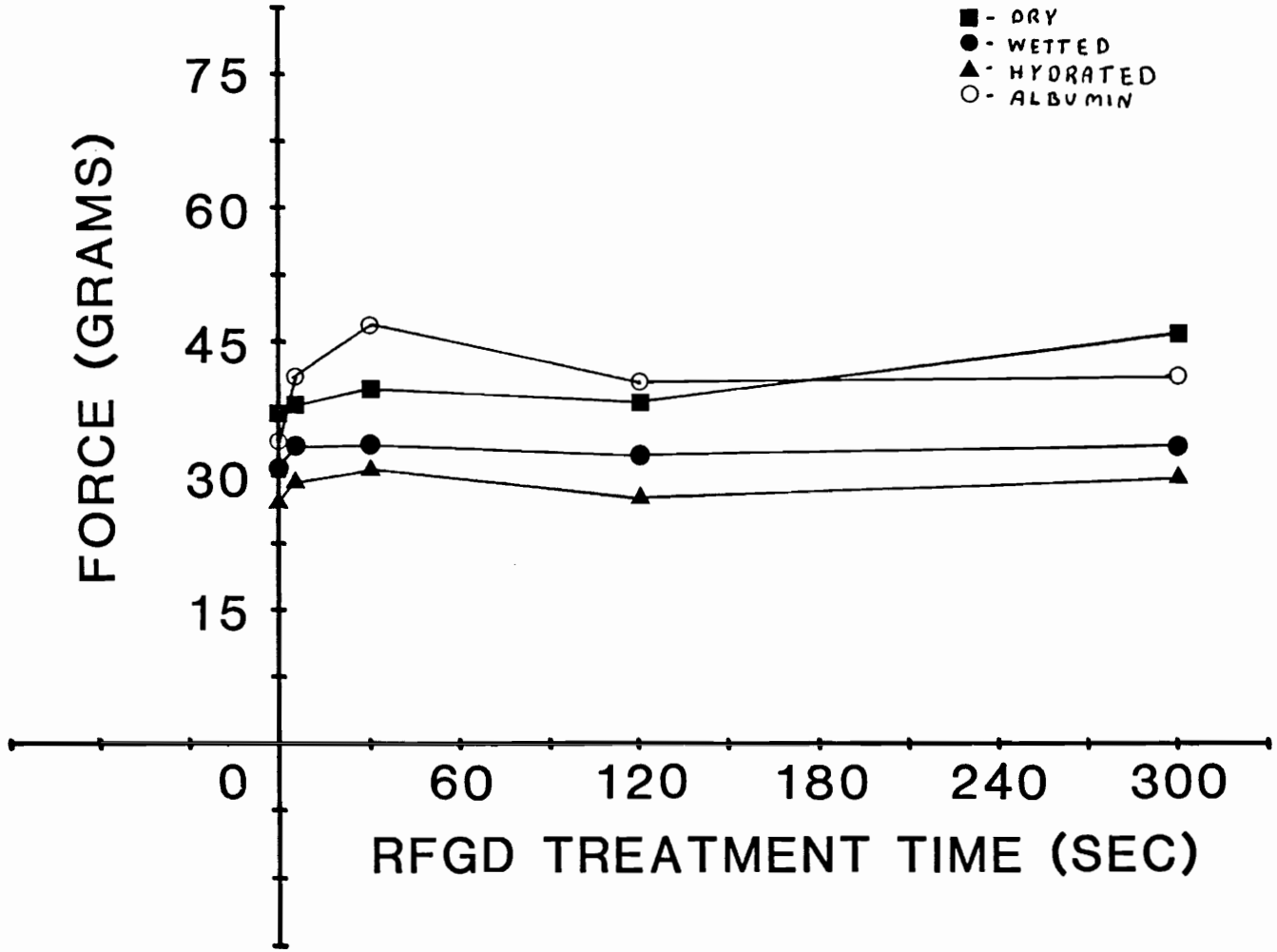

Figure 4.10 Friction as a function of radio frequency glow discharge treatment time for the polyethylene-Ducor polyurethane catheter pair, PE-PU_1

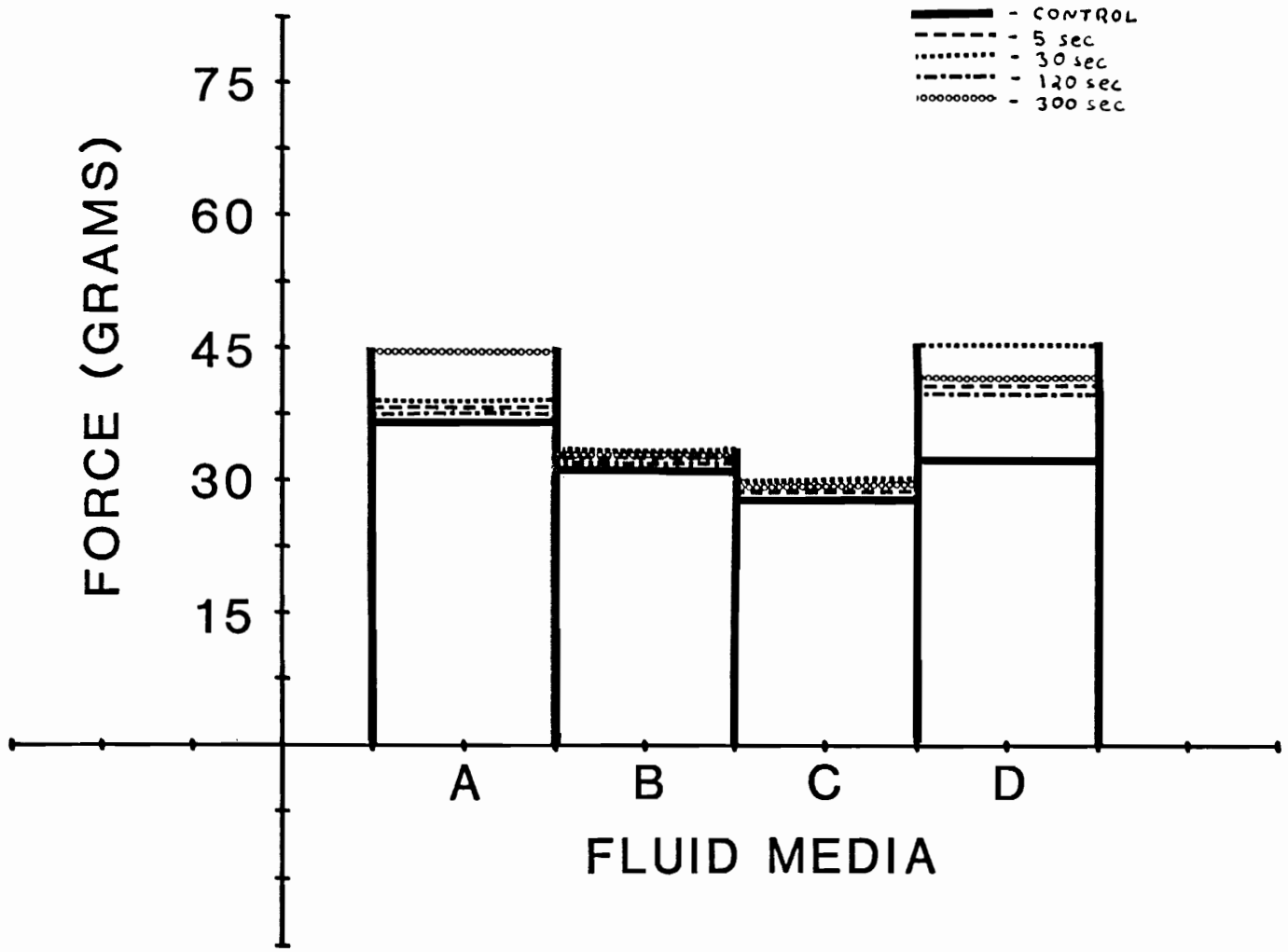

Figure 4.11 Friction as a function of the fluid media for the polyethylene-Ducor polyurethane catheter pair, PE-PU_1

4.3.3 Polyethylene-Polyurethane 2

This catheter pair behaved much like the previous pair. Figure 4.12 shows a relatively constant friction value for all RFGD treatment times. Figure 4.13 is much like Figure 4.11 for the PE-PU_1 in that the friction values decreased from the dry to the hydrated system, and increased to the albumin-treated catheter. In this case, a higher value than that of the dry system is acquired for all of the albumin systems.

This catheter pair exhibited predominately type "C" behavior with intermittent spikes occurring, expressing a more elastomeric nature than the polyurethane 1 pair. This is supported by the mechanical tests (Sec. 4.4) which revealed a lower tensile modulus for the PU_2 catheter than for the PU_1 catheter.

4.3.4 Polyethylene-Silicone Rubber

Table 4.4 and Figures 4.14 and 4.15 display the results procured for the PE-SR pair. Figure 4.14 exhibits much the same behavior as those previous, except in the dry case. For this case the friction rises initially, peaks at 30 seconds, and subsequently decreases to the 300-second point. Figure 4.15 shows a continual decrease of the friction for each of the fluids used, including the albumin.

The PE-SR pair displayed a combination of type "B" and "D" behavior. A slow rise time and sharp drop off was

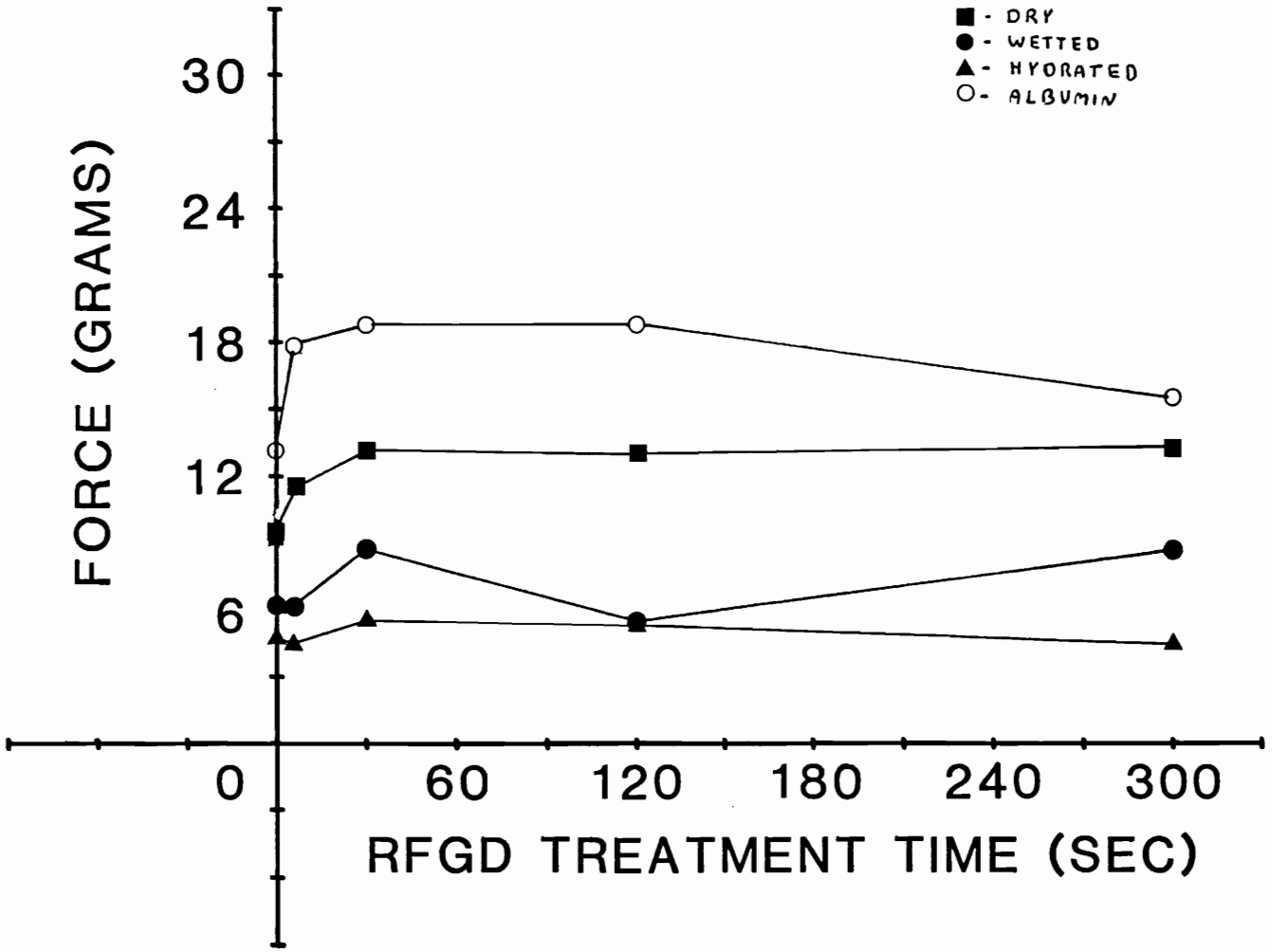

Figure 4.12 Friction as a function of the radio-frequency glow discharge treatment time for the polyethylene-B-D polyurethane catheter pair, PE-PU_2

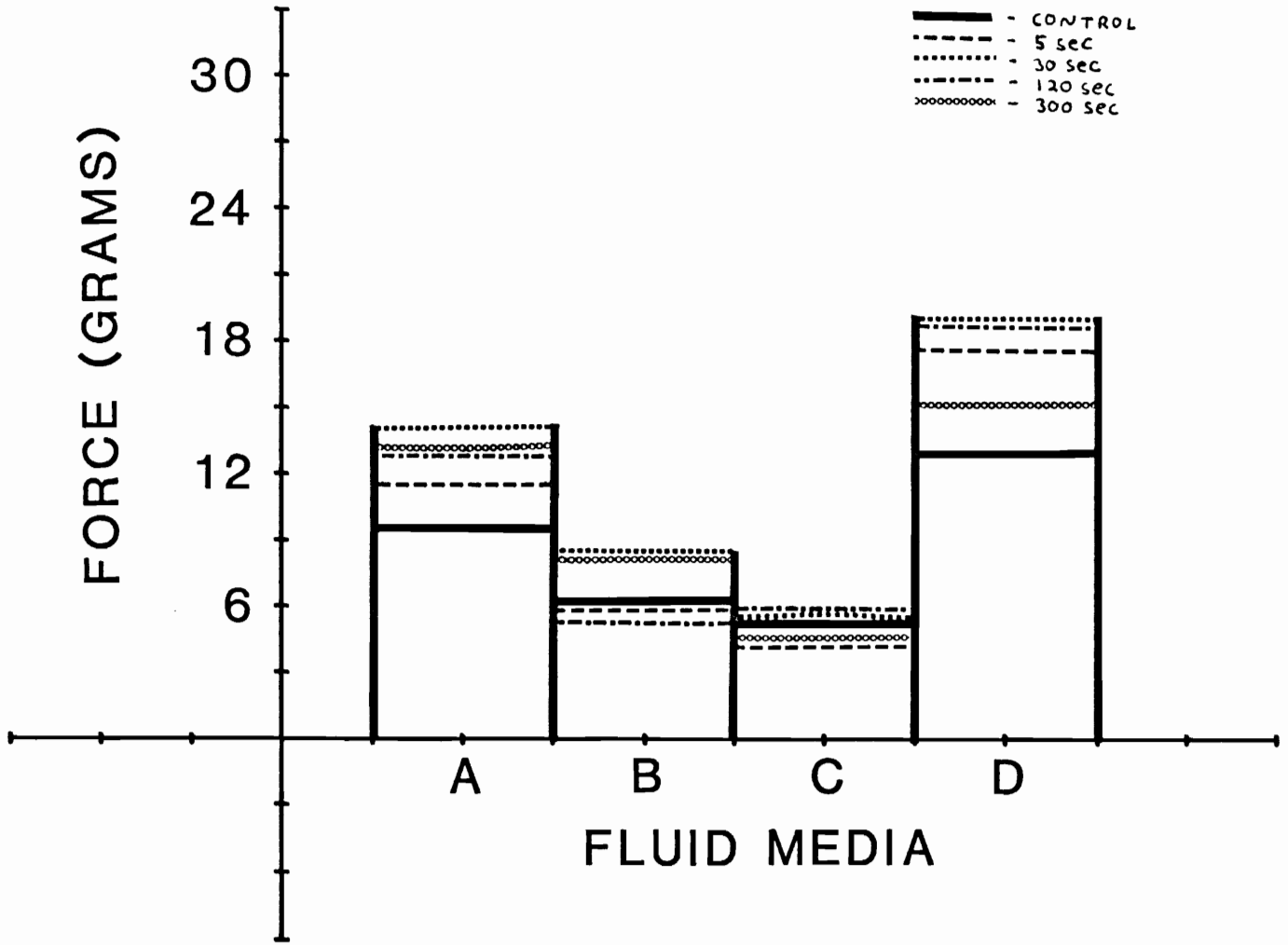

Figure 4.13 Friction as a function of the fluid media for the polyethylene-B-D polyurethane catheter pair, PE-PU_2

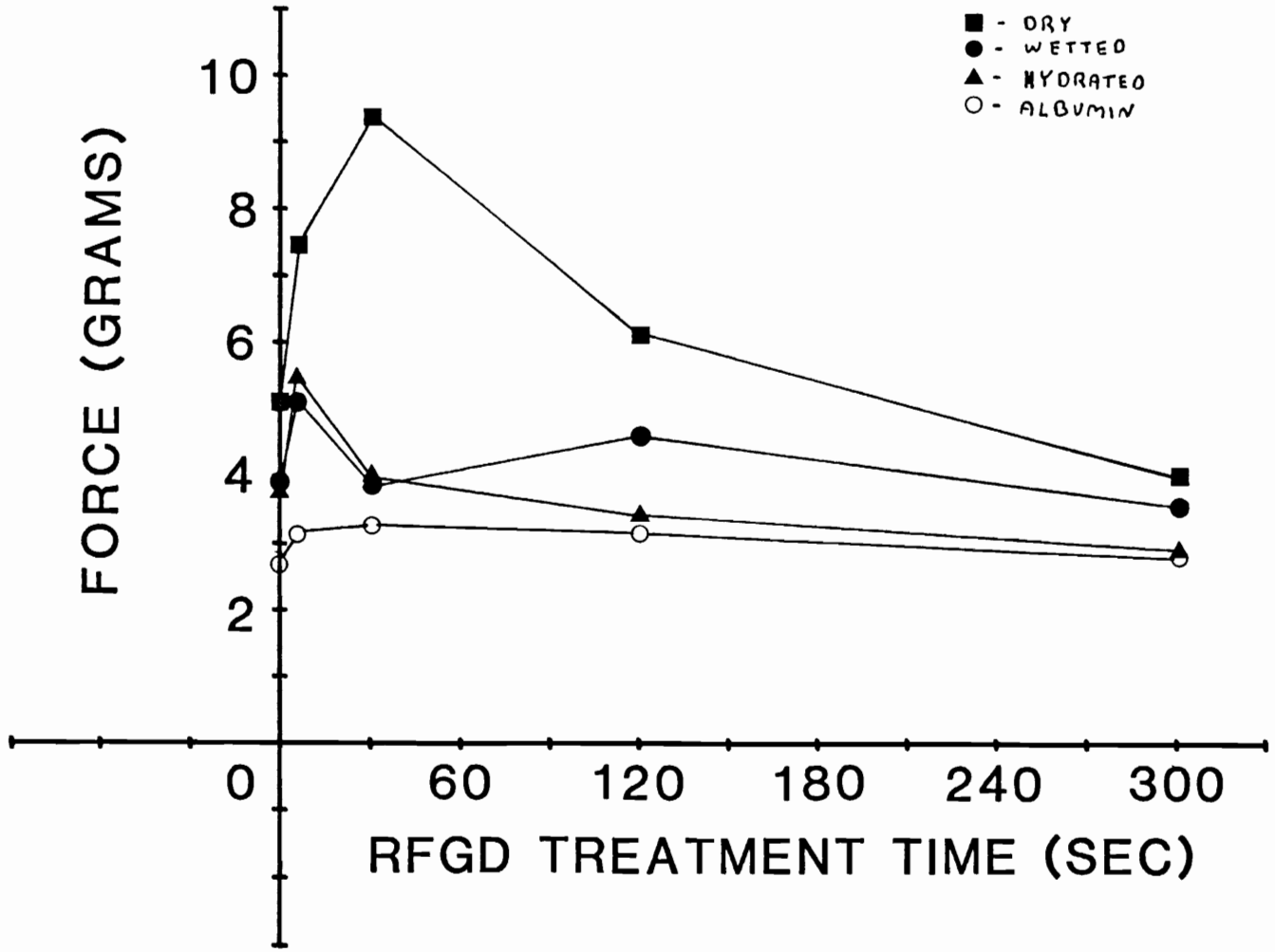

Figure 4.14 Friction as a function of the radio-frequency glow-discharge treatment time for the polyethylene-silicone rubber catheter pair, PE-SR

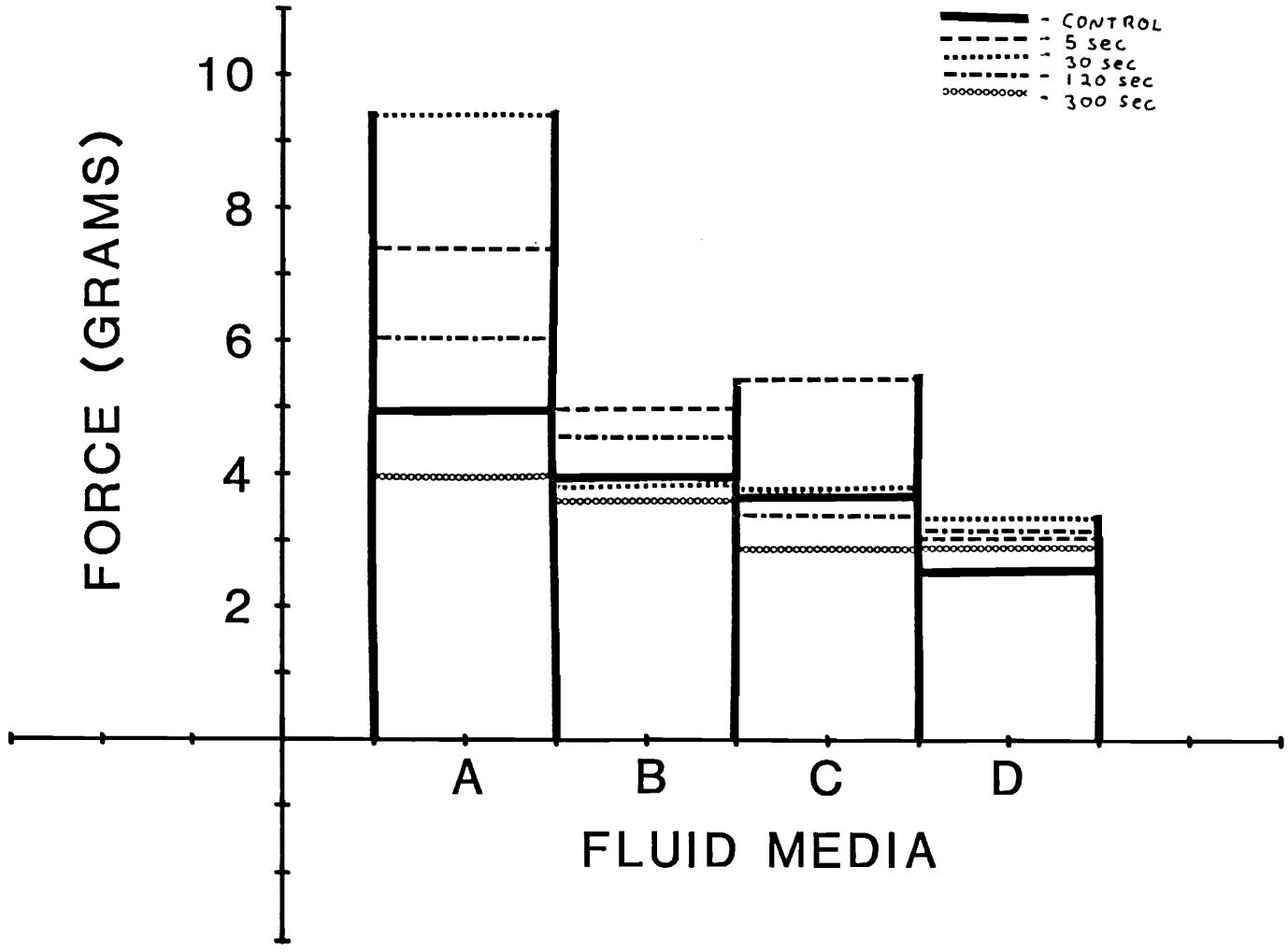

Figure 4.15 Friction as a function of the fluid media for the polyethylene-silicone rubber catheter pair, PE-SR

observed; the peaks were very small in amplitude, giving a relatively constant friction value as the silicone rubber catheter was being pulled.

4.3.5 Polyurethane-Polyurethane 1

Table 4.4 and Figures 4.16 and 4.17 show the outcome of this pair of catheters. With these catheters, there seems to be a significant effect of RFGD treatment on the friction values. As seen in Figure 4.16, the friction increases after 30 seconds at least back to, and even beyond, the value of the untreated catheter for all the fluids. The various fluid treatments produce much the same outcome as previously (Fig. 4.17), the main difference being a much sharper drop in friction from the dry to the wetted and hydrated systems. Although a sharp rise does occur from the hydrated to the albumin systems, the value never reaches that of the dry case.

This catheter pair exhibits type "A" behavior with very high frequency peaks of relatively high amplitude. The peaks remained relatively constant for both maximum and minimum values. An initial spike was observed at the beginning of each tracing, as in type "D" behavior.

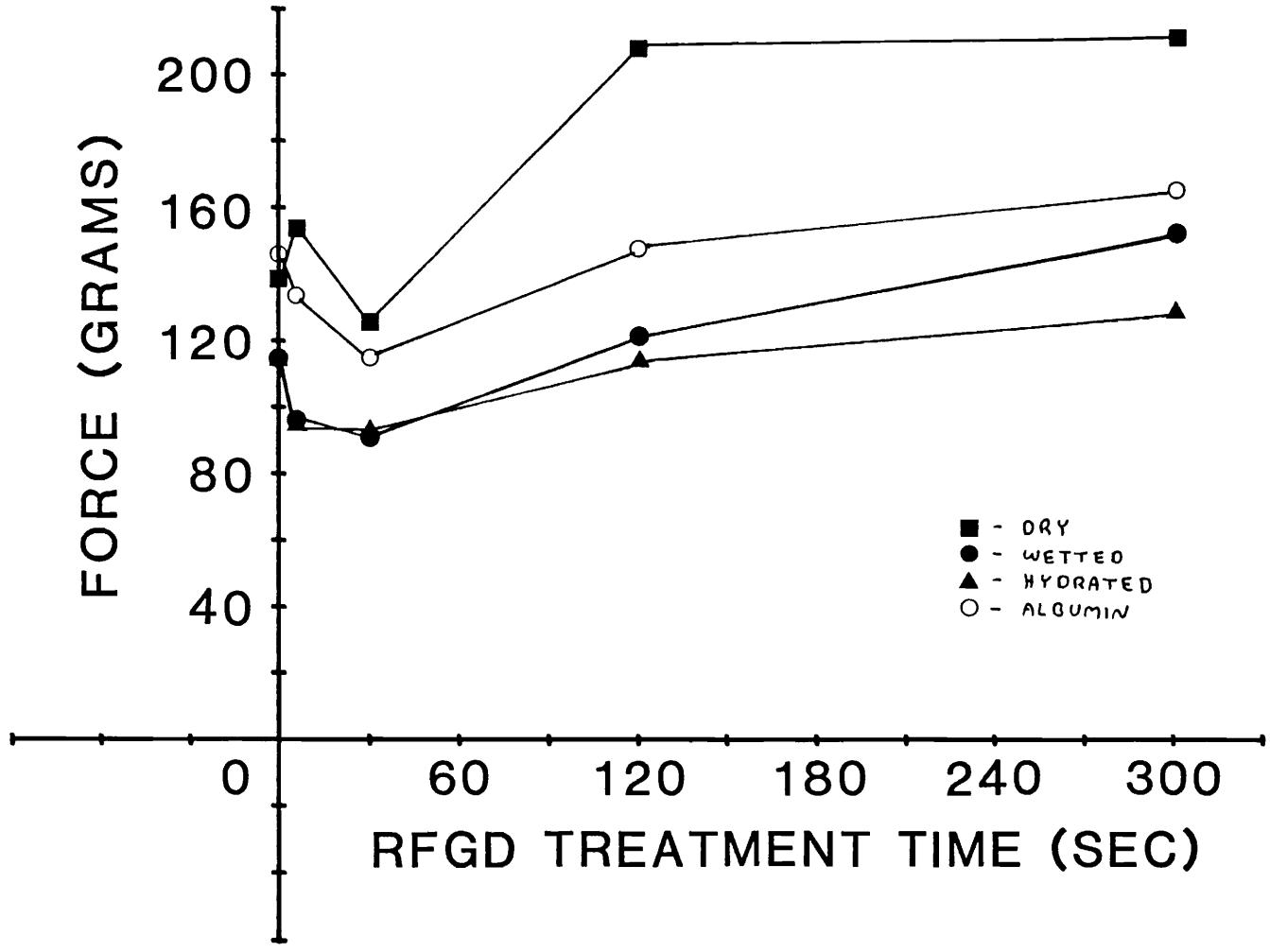

Figure 4.16 Friction as a function of the radio frequency glow discharge treatment time for the Ducor polyurethane-Ducor polyurethane catheter pair, $PU\text{-}PU_1$

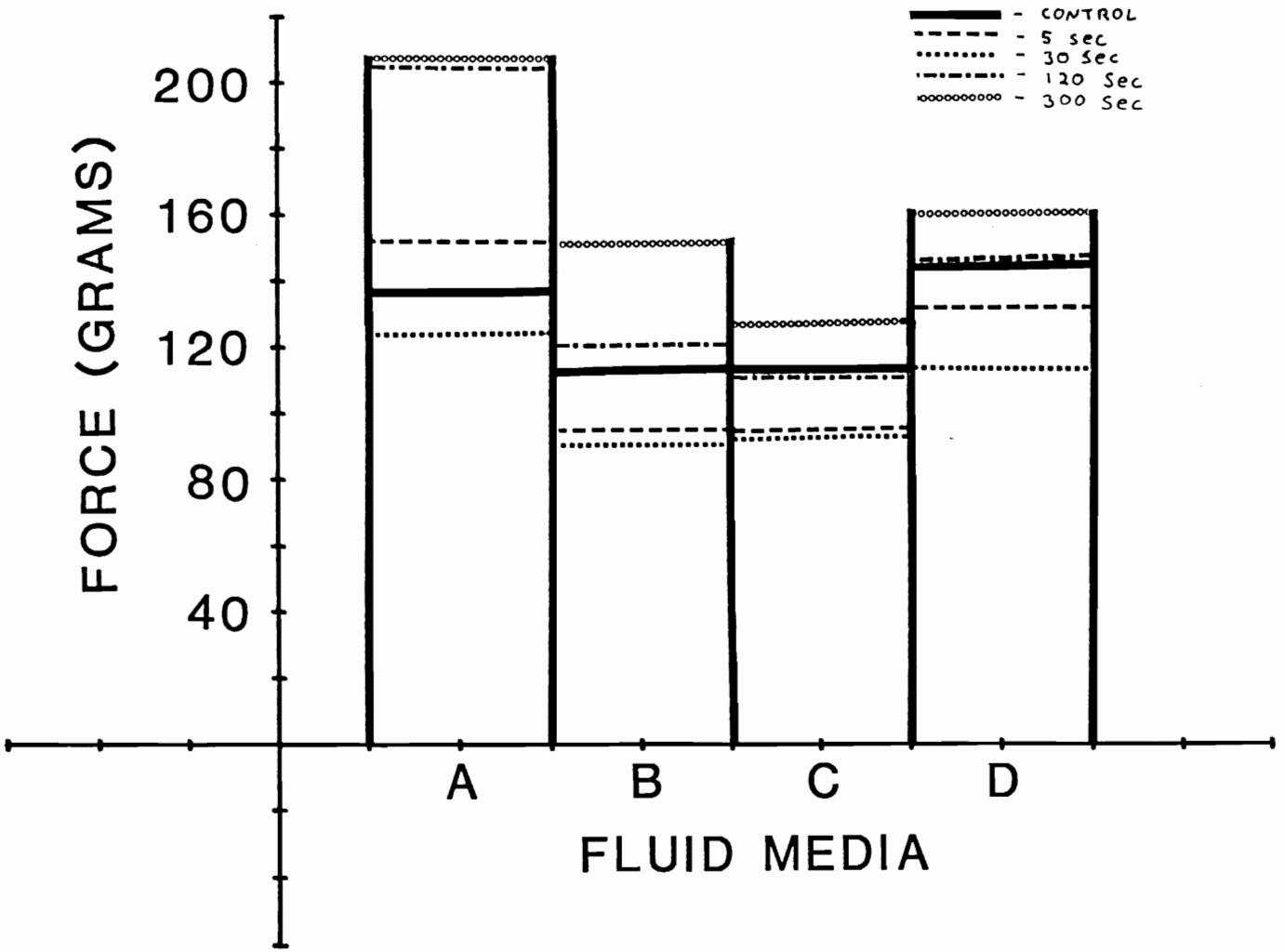

Figure 4.17 Friction as a function of the fluid media for the Ducor polyurethane-Ducor polyurethane catheter pair, PU-PU_1

4.3.6 Polyurethane-Polyurethane 2

Table 4.4 and Figure 4.18 show that for all fluids an initial decrease is observed from the untreated to the five-second point, after which each system varies with no correlation between RFGD treatment time and the friction observed. Figure 4.19 shows that, here again, the friction drops dramatically from the dry to the wetted system, and a large increase in friction from the hydrated to the albumin treatment.

This combination of catheters exhibited a very definite type "B" behavior. Long, slow rise times with very sharp drop offs occurred. The excursions from peak to trough were of very high amplitude. This suggests that the combination of the two polyurethanes causes the inner polyurethane catheter to express more of an elastomeric nature than it does with the polyethylene outer catheter.

4.3.7 Polyurethane-Silicone Rubber

The consequences of the PU-SR pair are shown in Table 4.4 and Figures 4.20 and 4.21. Except for the dry case, no effect of RFGD treatment is seen on friction. As can be seen from Figure 4.20 for the dry test, the initial response at 5 seconds of treatment was a slight decrease in friction, after which the value rose markedly to the 30-second point. Upon further RFGD treatment, the friction decreased rapidly to the 300-second point.

Figure 4.21 displays the effect of various fluids with the PU-SR pair. Unlike the PE-SR catheters, the

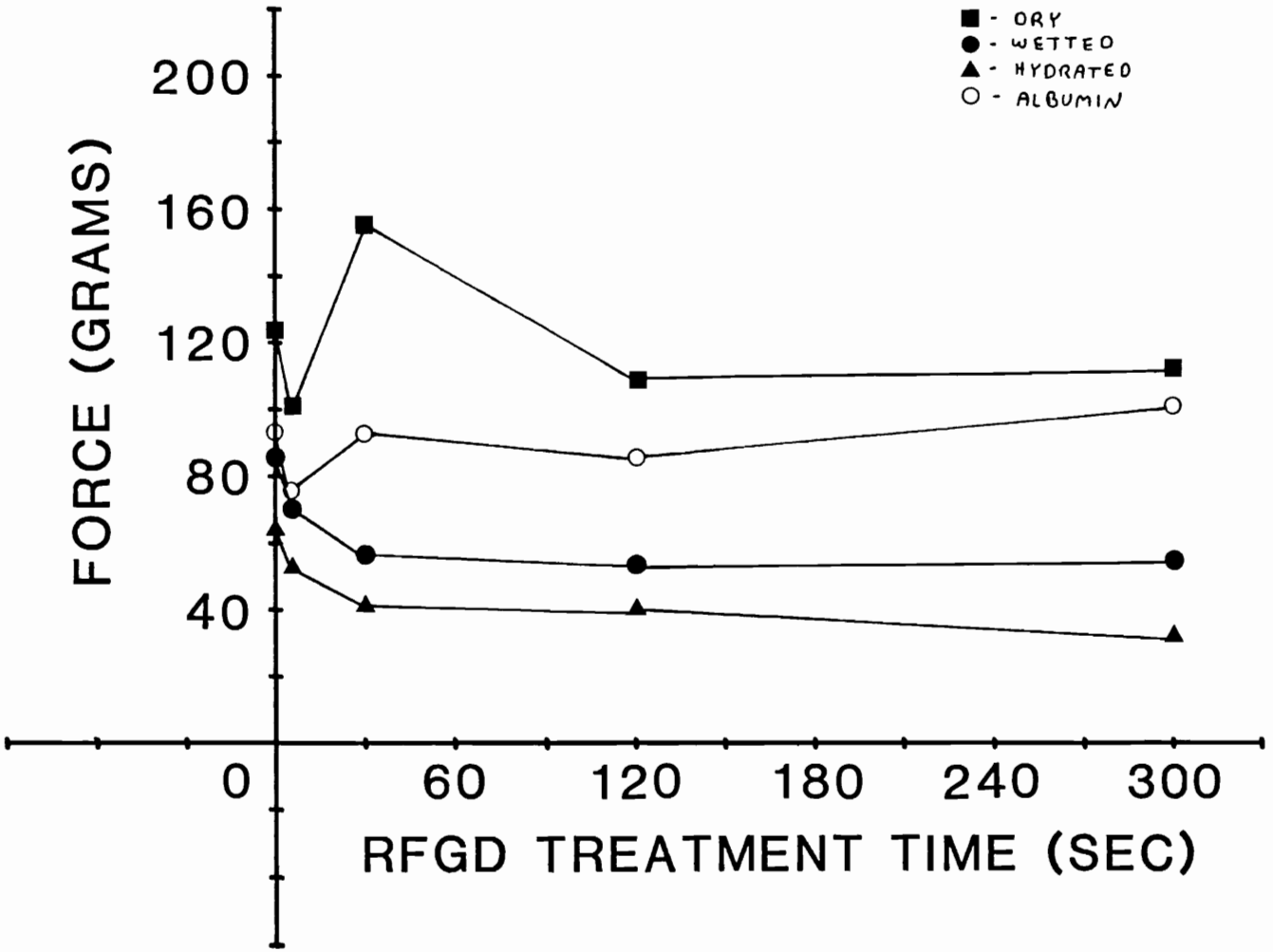

Figure 4.19 Friction as a function of the radio-frequency glow discharge treatment time for the Ducor polyurethane-B-D polyurethane catheter pair, PU-PU_2

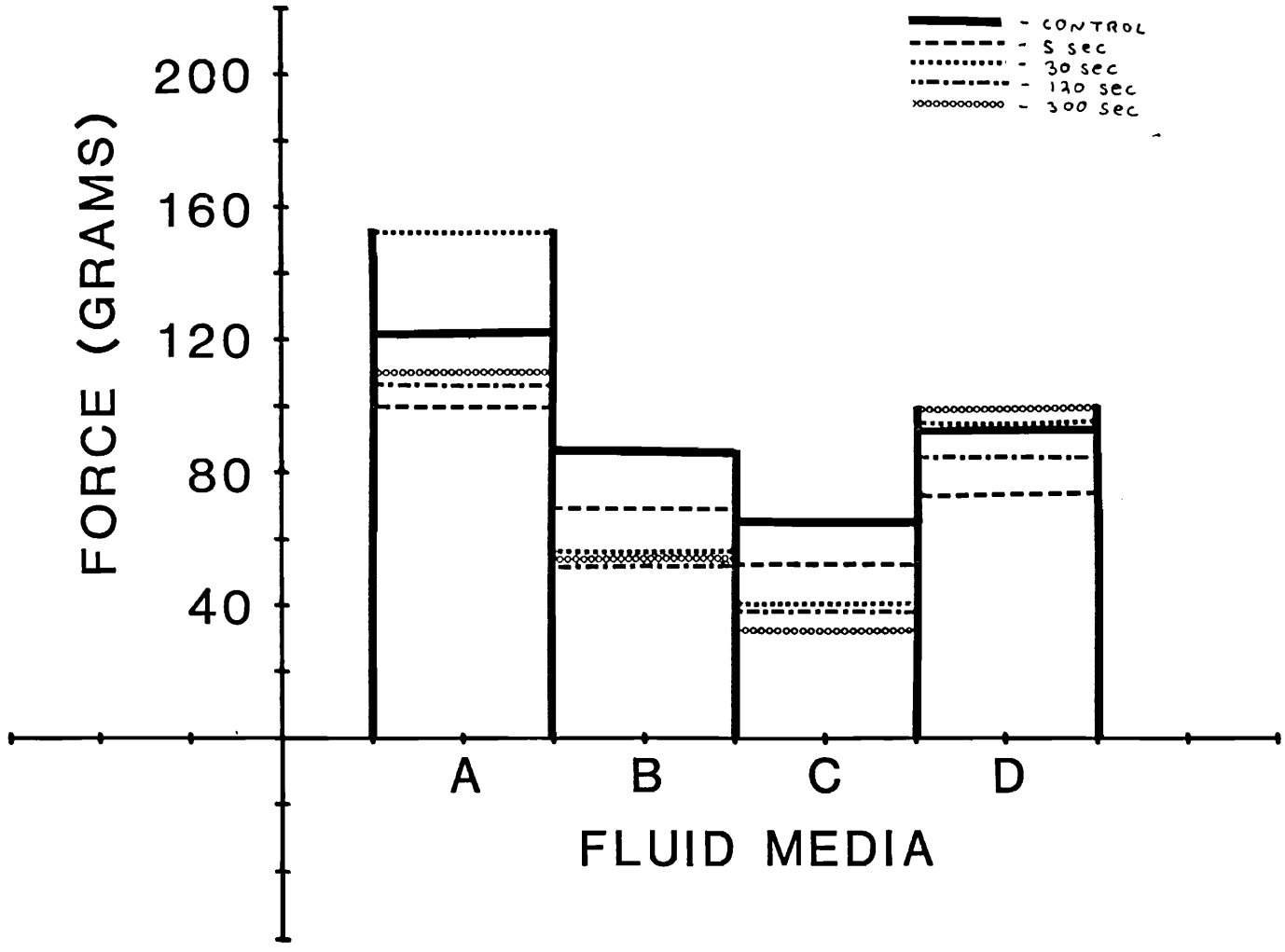

Figure 4.19 Friction as a function of the fluid media for the Ducor polyurethane-B-D polyurethane catheter pair, PU-PU_2

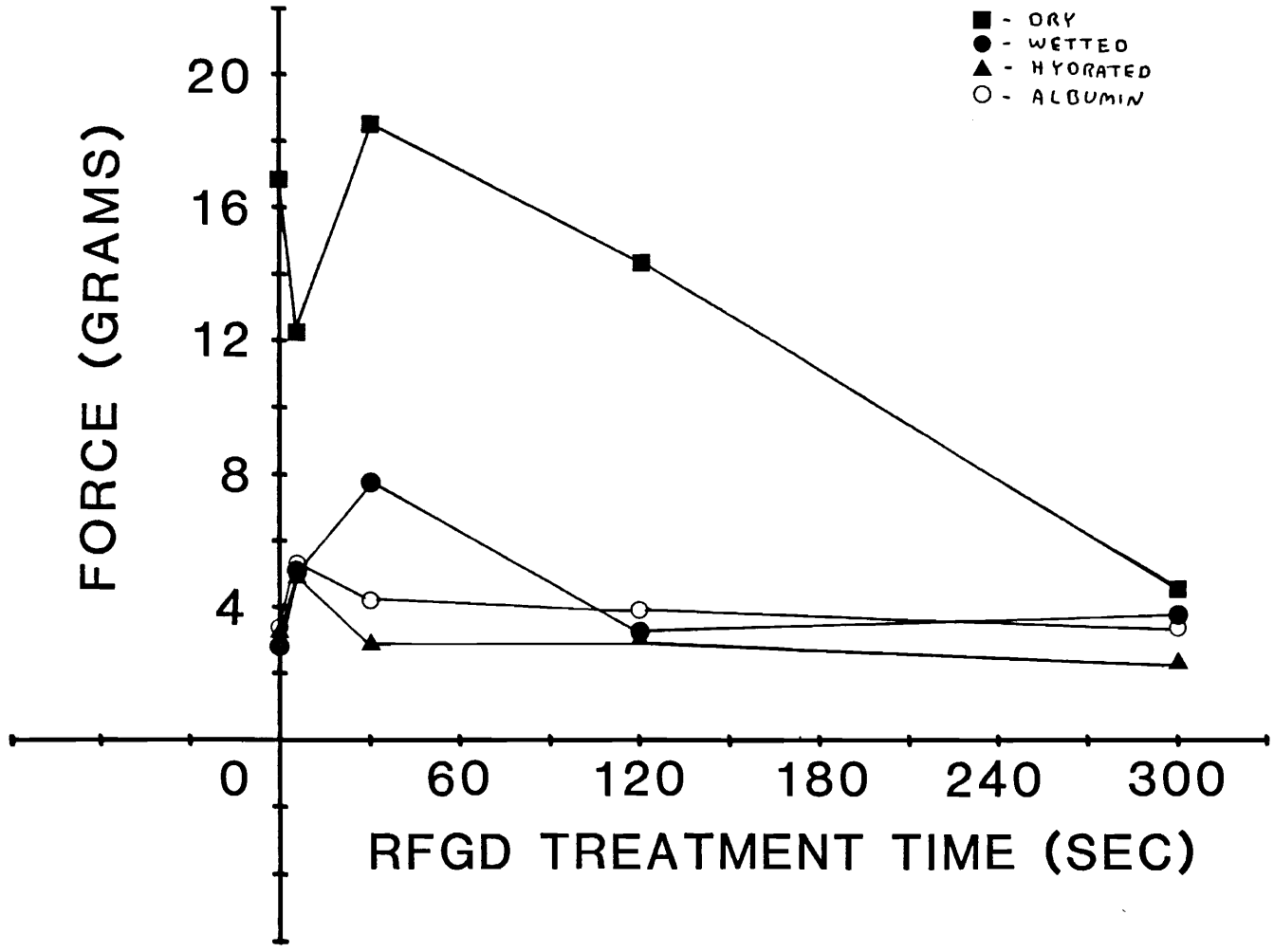

Figure 4.20 Friction as a function of the radio-frequency glow discharge treatment time for the Ducor polyurethane-silicone-rubber catheter pair, PU-SR

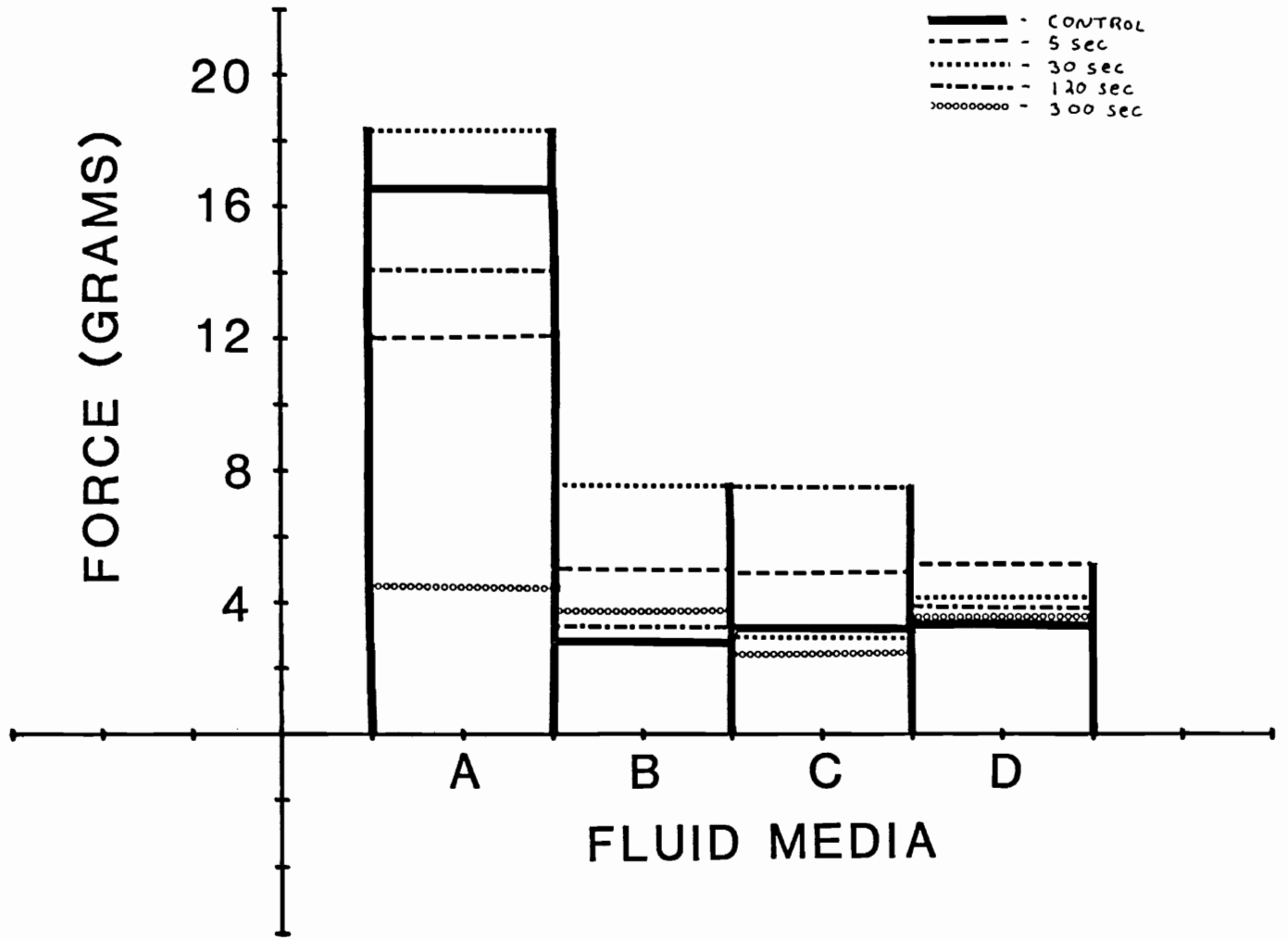

Figure 4.21 Friction as a function of the fluid media for the Ducor polyurethane-silicone rubber catheter pair, PU-SR

albumin treatment in this pair leads to a slight increase in friction over the hydrated system. Here, again, there is a drastic decrease from the dry to the wetted system.

The frictional behavior of this pair was highly dependent upon the fluid utilized. This is to be noted, since none of the other catheter pairs exhibited this dependency. For the dry systems, the behavior was predominantly "C" type, even though there were intermittent smooth sections on the tracings. As the catheters were wetted, the frictional behavior resembled that of type "D," yet with small amplitude peaks of constant value. The hydrated catheters displayed the same type of behavior as the wetted system, with slightly more "C" character, in that more peaks occurred at constant intervals and higher amplitude. The albumin systems were all of type "D," with smooth curves throughout.

It is believed that this dependency upon fluid is a result of the nature of the silicone rubber. As mentioned earlier, the silicone rubber seems to utilize the albumin, and also the PBS, to its advantage in decreasing the interfacial bonds between the silicone rubber and the other catheters employed.

4.3.8 Conclusions

The most obvious conclusions to be drawn from the above results are first, little or no effect of RFGD treatment on friction is observed, and second, the fluid

pretreatments show sometimes drastic effects on friction reduction. It may be inferred that a small friction increase takes place with a short, 5-second, treatment with the PE outer catheters since the majority of the results show this initial increase. This turns out to be statistically insignificant with a P value of $>.01$. With the PU outer catheter tests the data shows an initial decrease in the first 5 sec. This again proves to be statistically insignificant with a p value $>.05$. Triolo (38), in his experiments, did obtain significant reduction of friction upon RFGD treatment of pure, spincast polymers. Comparable studies done by Triolo on polyethylene vs. silicone rubber in distilled water (38), showed large decreases in friction with this polymer pair upon a 300 second RFGD treatment. Triolo's film thickness may have had an influence on the resultant friction decrease. The difference also may be due to the geometries used, flat plate versus coaxial, or it may be a result of the difference in the polymers used.

The outcome of various fluids utilized as pretreatments was noteworthy. For all of the catheter systems, excluding PE-PU_1, a decrease in friction of 30 to 50% occurred after the inner catheter was wetted in the PBS solution. Upon hydration for 4 hours in the PBS, a slight decrease occurred for all of the catheter pairs, and this decrease proved to be statistically significant ($P < .005$).

One of the most interesting outcomes of this study is the effect of albumin pretreatment on the friction. As

was seen with the PE-PU_2 catheter pair, the albumin data showed a consistently larger friction values than the dry system. For all catheter pairs, except PE-SR, the albumin pretreatment led to an increased friction value over the hydrated arrangement. The concentration of albumin used, 10 mg/ml, closely approximates that of actual human blood levels, 35-55 mg/ml (74). It may be, with clinical catheterization, that the albumin present in the blood aids in the increase of friction between the coaxial catheters, either due to interfacial interactions or increased viscosity. The other blood elements (red blood cells, platelets, etc.) may also play a large role in the friction, especially when coagulation occurs (Unpublished observation). This is not the case, of course, when the catheters are continually flushed out and kept clear of blood materials.

The reason behind the decreased friction values of the albumin treatment of the PE-SR system is worth investigating further. The interfacial friction between the polyethylene and the silicone rubber is obviously decreased with the albumin fluid. It is known (75-78) that albumin binds almost irreversibly to polyethylene and silicone rubber through hydrophobic interactions. It is also hypothesized that the albumin molecules line up in either an end to end or side by side fashion setting up a regular, symmetrical monolayer on the surface of the polymer. Since the largest hydrophobic region of the

albumin molecule is utilized in the bonding of the protein to the polymer, the hydrophilic region of the protein will be exposed, favoring a water layer on the hydrophilic surface of the protein monolayer. In the case of the polyurethane catheters, the larger, somewhat hydrophilic, soft ether component of the polymer, along with the hard segments of the material may make the bonding of the albumin less strong and more reversible. The hydrophilic polyurethanes most likely bind the albumin through electrostatic forces (75) with the hydrophilic region of the albumin. This may expose the hydrophobic region of the albumin leading to a monolayer with a small water component.

Classical fluid dynamics describes a shear stress, μ, occurring between a surface in relative motion with respect to an opposing surface and that opposing surface (79). This gradient of shear assumes a "no-slip" condition at each of the surfaces (79). This is the classical measurement of viscosity (80). If the boundary layer on either surface is not consistent with the "no slip" condition the gradient will be lessened and the shear stress diminished. The shear stress is an indirect measure of the dynamic friction between two surfaces and therefore, in this case, the friction would be reduced.

It may be hypothesized that the adsorption of albumin on a hydrophobic surface, such as the polyethylene and silicone rubber used in these experiments, which leads

to a water layer on the exposed hydrophilic regions of the albumin, may serve to reduce the friction by decreasing the shear stress gradient in the boundary layers of the two surfaces. This would also account for the increased friction observed with the polyurethanes upon albumin treatment because of the exposed hydrophobic regions of the albumin minimizing the water layer and possibly maximizing the shear stress and, consequently, the friction.

This argument would also suffice to explain the intermediate friction change obtained with the PU-SR system. The silicone rubber will bind the albumin in such a way as to decrease the shear stress at its surface, whereas the polyurethane acts to increase its shear stress at the surface thereby cancelling out the two effects and providing little or no friction change from the hydrated value.

As the carbon-oxygen ratios and atomic percent oxygen remained constant with the polyurethane inner catheters, upon treatment with RFGD, no correlations could be determined between carbon-oxygen ratios and friction. For the silicone rubber catheters, even though the carbon-oxygen ratio varied, no correlation could be determined. The same held true for contact angle versus friction.

4.4 Mechanical Tests

Four to six tests were performed on each of the three inner catheters, and the values compared with those in the literature. For the PU_1 catheters, the tensile modulus obtained was $3.6 \times 10^4 \pm 4.7 \times 10^3$ PSI. The literature values (71) for polyurethanes range from 1×10^4 to 3.5×10^5 psi. The value obtained in these tests is therefore within the range of those in the literature. Since the values are in the lower range of the literature values, it is assumed that these catheters are comparably more elastomeric.

The PU_2 catheter showed a lower tensile modulus than did the PU_1 catheter. The average value of six tests gave $2.4 \times 10^3 \pm 4.5 \times 10^2$ psi. Again, this value is on the low end of the literature values, inferring a catheter with an elastomeric nature. Both of these polyurethane catheters displayed elastomeric friction behavior of type "C," demonstrating a stick-slip friction which may not have been as predominant if the catheters expressed a higher tensile modulus.

The silicone rubber catheters gave an average value over four tests of 31.1 ± 15.1 psi. The values reported in the literature depend heavily upon the nature of the silicone rubber used. Most silicone rubbers are filled with silica, graphite, or other reinforcing material. These fillers give the material the strength desired for a

particular application. The literature values (81) therefore range from 1 to 100 psi.

4.5 In Vivo Tests

The results of the study done in the hepatic artery of a dog were inconclusive. The many uncontrollable variables made any quick quantitative tests very difficult. These variables included the wedging of the outer catheter's tip against the wall of the blood vessel at the point of the turn into the smaller vessel. As this occurs, it would hinder the path of entry of the smaller catheter into the larger catheter, resulting in erroneous force measurements.

A second variable which needed to be considered is that of arterial blood flow in the artery. These tests are done with live animals, and therefore large arterial pressures make the friction data false by introducing an increase in resistance (blood flowing away from the catheter junction), or actually pushing the inner catheter back out of the outer catheter. The latter actually occurred. When the catheters were placed in the aorta from the femoral artery, the inner catheter was forced rapidly out of the outer catheter, due to the extreme aortic pressure.

Other uncontrollable variables included constant coagulation of blood (even though the animal was more than adequately heparinized), control of position of the

catheter within the artery, reproducible placement of the outer catheter in the hepatic artery, and patency of the vessel upon constant intrusion by the catheters. Before any quantitative study on friction of coaxial catheters in vivo could be attained, all these variables would have to be controlled or otherwise eliminated. Since this was a piggyback study, no further attempts were made to minimize the affects of the variables and the study was therefore discontinued.

CHAPTER 5

CONCLUSIONS AND RECOMMENDATIONS FOR FUTURE WORK

Radio frequency glow discharge treatment of polyurethane catheters for times of 0, 5, 30, 120, and 300 seconds showed no evidence of oxidation of the surface, as seen with XPS. A degradation of the polymer seems to take place over the treatment time. This degradation could be either a photodegradative process or it could be surface chemical reactions, and should be further investigated. X-ray photoelectron spectroscopy of the silicone rubber catheters shows definite oxidation of the surface. The type of oxygen moieties obtained needs to be looked at in more detail to determine the relationship between the oxidation and contact angle or friction data. The XPS data also show a continuing increase in oxygen present as treatment time continues. It may therefore be possible to further oxidize the surface with RFGD treatment times longer than five minutes.

The contact angle data shows that RFGD treatment makes all of the polymer surfaces more hydrophilic within the first 30 seconds. This may be the result of oxidation, as with silicone rubber, or it may be due to a rearrange-

ment of the surface chemistry to create a more polar surface, as with the polyurethanes. Hydration of similar polymers and subsequent contact angle analysis showed no significant effects on the surface energy of the material (38).

The friction analysis may best be summarized by saying that RFGD treatment does little or nothing to reduce friction with these catheter materials, whereas the use of various fluids as pretreatment and testing media produces marked friction reduction. The most significant outcome of this investigation is the increased lubricity obtained upon treatment of the silicone rubber catheters in an albumin solution. An in-depth analysis of this phenomenon is warranted. It would be advisable to do a pretreatment of all these catheters in an albumin solution and subsequently wash the catheters to look at protein adsorption with XPS or other means, to determine how the protein aids in the process of friction reduction. Running the friction tests after the adsorption of albumin in dry, PBS, or even saline solutions, would be the next step in the determination of the mechanism of this friction reduction.

Although RFGD treatment exhibits no effect on the resultant friction, it may be that treatment of the outer catheter's luminal surface might aid in the reduction of friction. This could be done by using the lumen of the outer catheter as a plasma chamber. It could be evacuated, then treated by passing a radio-frequency coil over the

catheter, thereby treating the luminal surface.

Triolo (38) suggests variable cross-linking of the materials, in particular SR, to assess the chemical versus mechanical contributions to friction. A study of the effects of RFGD treatment on the thrombogenic nature of the catheters would also be worth pursuing. Work by Smith (82) and others has demonstrated good correlation between biological cell adhesion to surfaces and their contact angle measurements. Triolo (38) showed that platelet adhesion occurred less to the oxidized polymers than to the control surfaces. This may suggest that the oxidized surfaces may be more blood compatible. This needs to be examined in vivo.

Other avenues to obtain friction reduction in coaxial catheters need to be pursued. It may be advantageous to employ chemical lubricants, such as glycoasaminoglycans, in these systems. Glycoasaminoglycans are used in nature to reduce friction between two surfaces, as seen with hyaluronic acid in the synovial fluid of the knee. These mucopolysaccharides could be covalently or ionically bound to the surface of the polymer, thereby reducing or eliminating contact between polymers, resulting in reduction of the frictional components.

More inner (small diameter) catheters need to be investigated. To this point, very few materials are utilized in the manufacture of these smaller catheters, as

the market has not yet opened to this technology. A more thorough look at the different material responses to all of the aforementioned techniques for friction reduction would be merited.

REFERENCES

1. J. M. Steckelbers, R. E. Vliestra, J. Ludwig, and R. J. Mann, "Werner Forssmann (1904-1979) and His Unusual Success Story," Mayo Clinic Proceedings, 54, 746-748 (1979).

2. A. Cournand, and H. A. Ranges, "Catheterization of the Right Auricle in Man," Proc. Soc. Exp. Biol. and Med. 46, 462 (1941).

3. J. D. Richardson, F. L. Grover, and J. K. Trinkle, "Intraveneous Catheter Emboli," The American Journal of Surgery, 128, 722-727 (1974).

4. J. A. Ryan, Jr., R. M. Abel, W. M. Abbott, C. C. Hopkins, T. M. Chesney, R. Colley, K. Phillips, and J. E. Fischer, "Catheter Complications in Total Parenteral Nutrition," N. Engl. J. Med., 290, 757 (1974).

5. J. W. Broviac, J. J. Cole, and B. H. Scribner, "A Silicone Rubber Atrial Catheter for Prolonged Parenteral Alimentation," Surg., Gynecol., Obstet., 136, 602 (1973).

6. M. Clark and D. Shapiro, "Substituting Catheters for Scapels," Newsweek, Oct. 30, 111 (1978).

7. D. Curran, "Application of Noradrenalin for Mallory-Weiss Bleeding Lancet 1:538, 8167 (1980).

8. J. B. Downs, R. L. Chapman, Jr., and I. F., Hawkins "Prolonged Radial-Artery Catheterization: An Evaluation of Heparinized Catheters and Continuous Irrigation" Arch. Surg., 108, 671 (1974).

9. A. Kopman, "Hemoptysis Associated with the Use of a Flow-Directed Catheter," Anesth. and Analg., 58, 153 (1979).

10. R. S. Baigrie, et al., "Hemodynamic Monitoring: Catheter Insertion Techniques, Complications and Trouble Shooting," CMA Journal, 121:7 885 (1979).

11. H. J. C. Swan, " Balloon Flotation Catheters," J. Am. Med. Assoc., 233, 865 (1975).

12. J. T. Shepherd, "The Cardiac Catheter and the American Heart Association," Circulation, 50, 418 (1974).

13. M. H. Whaley, "Technology of Balloon Catheters in Interventional Angiography," Radiology, 125, 671 (1977).

14. A. Berenstein, and I. I. Kricheff, "Catheter and Material Selection for Transarterial Embolization: Technical Considerations," Radiology, 132, 631 (1979).

15. R. I. White Jr., S. L. Kaufman, K. H. Barth and J. D. Strandberg, "Therapeutic Embolization with Detachable Silicone Balloons," J. Am. Med. Assoc, 241, 1257 (1979).

16. R. L. Fisher, "Progress in the Medical Management of Gallstones," Med Times 107:2, 30 (1979).

17. G. B. Kolata, "New Treatment for Coronary Artery Disease," Science, 206, 917 (1979).

18. Federal Register - Part II, Dept. of HEW-FDA, "Cardiovascular Devices: Classification and Development of General Provisions," Feb. 5, 7910-7916 (1980).

19. D. B. Cotton, and T. J. Benedetti, "Use of the Swan-Gamz Catheter in Obstretics and Gynecology," Obstet. and Gynecol., 56:5 641 (1980).

20. J. B. Dietrich, "Outpatient Cardiac Catherization and Arteriography: Twenty Month Experience at the Arizona Heart Institute," Cardiovascular Diseases, 8, no. 2, 195 (1981).

21. S. E. Mitchell, and R. A. Clark, "Complications of Central Venous Catheterization," Am. J. Rad., 133, 467 (1979).

22. G. A. Foote, S. I. Schabel, and M. Hodges, "Pulmonary Complications of the Flow Directed Balloon-Tipped Catheter," N. Eng. J. Med., 290:17 927 (1974).

23. J. F. Greene Jr., J. E. Fitzwater, and T. P. Clemmer, "Septic Endocarditis and Indwelling Pulmonary Artery Catheters," J. Am. Med. Assoc., 233, 891 (1975).

24. J. H. Henzel and M. S. DeWeese, "Morbid and Mortal Complications Associated with Prolonged Central Venous Canulation," Am. J. Surg., 122, 600 (1971).

25. J. F. Hicker, G. C. Fish, and P. C. Farrell, "Measurement of Thrombus Formation on Intravascular Catheters," Anesth. and Int. Care, 4:3, 1976.

26. F. H. Yarra, R. Oblath, H. Jaffe, D. H. Simmons, and S. E. Leny, "Massive Thrombosis Associated with the Use of the Swan-Gamz Catheter," Chest, 65:6, 682 (1974).

27. G. Formanek, R. S. Frech, K. Amplatz, "Arterial Thrombus Formation During Clinical Percutaneous Catheterization," Circulation, 41, 833 (1970).

28. A. G. Keresteci, "Indwelling Catheter Infection," CMA Journal, 109, 711 (1973).

29. J. D. Band and D. G. Maki, "Infections Caused by Arterial Catheters Used for Hemodynamic Monitoring," Am. J. Med. 67, 735 (1979).

30. A. E. Becker, M. J. Becker, F. H. Martin, and J. E. Edwards, "Bland Thrombosis and Infection in Relation to Intracardiac Catheter," Circulation, 46, 200 (1972).

31. T. T. Bashour, T. Banks and T. O. Cleng, "Retrieval of Lost Catheters by a Myocardial Biopsy Device," Chest, 66, 395 (1974).

32. G. W. Welch, D. W. McKeel Jr., P. Silverstein, and H. L. Walker, "The Role of Catheter Composition in the Development of Thrombophlebitis," Surg. Gynecol. and Obstet., 138, 421 (1974).

33. J. D. Bloom, "Defective Limb Growth as a Complication of Catheterization of the Femoral Artery," Surg. Gynecol. and Obstet., 138, 524 (1974).

34. F. E. Johnson, D. S. Summer, and D. E. Standness, "Extremity Necrosis Caused by Indwelling Arterial Catheters," Am. J. Surg. 131, 375 (1976).

35. F. J. Miller Jr., "Delivery Systems for Low Viscosity Silicone Rubber Through Small Co-Axial Catheters," Radiology, 131:2, 538 (1979).

36. W. Ganz, et al., "Intracoronary Thrombolysis in Evolving Myocardial Infarction," Am. Heart Journal, 101:1, 4 (1981).

37. J. W. Boretos, R. M. Terek, M. E. Girton, and J. L. Dippman, "Cohesive and Frictional Reduction in Intra-Arterial Microcatheters," 33rd ACEMB 30 Sept. - 30 Oct. 1980.

38. P. Triolo, "Surface Modification and Characterization of Some Commonly Used Catheter Materials," Master's Thesis, University of Utah, 1980.

39. Modern Plastics Encyclopedia, Modern Plastics Publishers, Oct. 1982.

40. G. R. Lappin, "Ultraviolet-Radiation Absorbers," Encyclo. Polymer Sci, and Tech., 14, 125 (1971).

41. J. J. Bernardo, and H. Burrell "Plasticization," Polymer Science, 1, 538 (1972).

42. J. H. L. Henson, and A. Whelan, Developments in PVC Technology, Wiley 1972.

43. F. W. Billmeyer, Textbook of Polymer Science 2nd Edition 379, Wiley-Interscience 1970.

44. A. Noshay and J. E. McSmith, "Review of Urethanes" in Block Copolymers: Overview and Critical Survey Academic Press 1977.

45. R. van Noort, M. M. Black, and B. Harris, "Developments in the Biomedical Evaluation of Silicone Rubber," J. Mat. Sci., 14, 197 (1979).

46. T. Kusano, K. Kobayaski, and K. Murakami, "Mechanical Chain - Scission in Rubber Vulcanizate at Low Temperatures," Rubber Chem. Technol. 52:4 773-780 (Sept.-Oct. 1979).

47. D. T. Clark, A. Dilks, and D. Shuttleworth, "The Application of Plasmas to the Synthesis and Surface Modification of Polymers," in Polymer Surfaces (D. T. Clark and W. J. Feast, Eds.), Chapt. 9 Wiley 1978.

48. J. R. Hollahan, Chemical Instrumentation: XXVII. Analytical Applications of Electrodelessly Discharged Gasses S. Z. Lewin ed. 1968.

49. J. R. Hollahan and G. L. Carlson, "Hydroxylation of Polymethylsiloxane Surfaces by Oxidizing Plasmas," J. Appl. Polymer Sci., 14, 2499 (1970).

50. C. A. L. Westerdahl, J. R. Hall, E. C. Schramm, and D. W. Levi, "Gas Plasma Effects on Polymer Surfaces," J. Colloid and Interface Sci., 47:3, 610 (1974).

51. R. E. Byer, Calspan Report.

52. D. J. Carlson and D. M. Wiles, "The Photodegradation and Photostabilization of Polymers, A Review," Rad. Curing, 3, 2 (1975).

53. B. J. Briscol, D. Tabor, Polymer Surfaces (D. T. Clark and W. J. Feast eds.) Chapt. 1 Wiley 1978.

54. A. Schallamack, " Anisotropic Rubber Friction Wear, 35:2, 375 (1975).

55. A. D. Roberts, "Adhesion and Friction of Celastomers," Rubber Chemistry and Technology, 54:5, 944 (1981).

56. J. W. Boretos, "Hydrogel Coating of Polyurethane for Increased Surface Lubricity," Transactions of Seventh Annual Meeting of the Society for Biomaterials, 1978.

57. V. Lindahl, and M. Hook, "Glycosaminoglycans and Their Bonding to Biological Macromolecules," Ann. Rev. Biochem, 47, 385 (1978).

58. D. T. Clark, W. J. Feast, "Application of Electron Spectroscopy for Chemical Applications (ESCA) to Studies of Structure and Bonding in Polymeric Systems," J. Macromal. Sci. - Revs. Macromal. Chem. C12:2 191 (1975).

59. L. T. Ngugen, N. H. Sung, and N. P. Suh, "Determination of Optimum Glow Discharge Parameters Based on ATR-FTIR Spectra," J. Polymer Sci.: Polymer Letters Edition, 18, 541 (1980).

60. H. Yosuda, H. C. Marsh, "ESCA Study of Polymer Surfaces Treated by Plasma," J. Polymer Sci.: Polymer Chemistry Edition, 15, 991 (1977).

61. D. T. Clark, A. Dilks, "ESCA Applied to Polymers," J. Polymer Sci.: Polymer Chemistry Edition, 16, 911 (1978).

62. C. S. Fadley, "Basic Concepts of X-ray Photoelectron Spectroscopy," from Electron Spectroscopy Theory, Techniques and Applications, (C. R. Brundle and A. D. Baker Eds.) Vol. 2, Chapt. 1, Pergamon Press (1978).

63. C. J. Powell, "The Physical Basis for Quantitative Surface Analysis by Auger Electron Spectroscopy and X-Ray Photoelectron Spectroscopy," from Quantitative Surface Analysis of Materials N.S. McIntyre, Ed., 5 (1978).

64. R. E. Johnson and R. H. Dettre, "Wettability and Contact Angles," in Surface and Colloid Science, 2, 3. Matijevic, Ed., Wiley 85 (1969).

65. I. Langmuir, "Overturning and Anchoring of Monolayers," Science, 87, 493 (1938).

66. L. Smith, C. Doyle, D. E. Gregonis, J. D. Andrade, "Surface Oxidation of Cis-Trans Polylutadiene," J. of Appl. Polymer Sci., 26, 1269 (1982).

67. J. H. Scofield, "Theoretical Photoionization Cross-sections in the 100-1500 eV Range. J. Electron Spectr. Rel. Phen, 8, 129 (1976).

68. R. J. Baird, "Variable Angle X-ray Photoelectron Spectroscopy," Ph.D. Thesis, University of Hawaii (1977).

69. C. D. Wagner, L. E. Davis, and W. M. Riggs, "Energy Dependence of the Electron Mean Free Path" Surface Interfact Analysis, 2, 53 (1980).

70. S. M. Hall, J. D. Anchade, S. M. Ma and R. N. King, "Photoelectron Mean Free Paths in Barium Stearate Layers," J. of Elec. Spectr. Rel. Phen, 17, 181-189 (1979).

71. J. H. Saunders, "Polyurethanes: Chemistry and Technology," Interscience Publishers (1969).

72. P. Feneberg and U. Krekeler, U.S. Patent 3,959,105 (1976).

73. L. M. Smith, Personal Communication, Report to NIH, (1980).

74. C. W. Blissit, O. L. Webb and W. F. Stanaszek, "Laboratory Diagnosis," from Clinical Pharmacy Practice, Chapt. 7 Lea and Febiger, Philadelphia (1972).

75. E. Brynada, M. Houska, Z. Pokoma, N. A. Cepalova, Y. V. Maiseeu, and J. Kalal, "Irreversible Adsorption of Human Serum Albumin onto Polyethylene Film," J. of Biorg., 2, 411 (1978).

76. E. Brynda, M. Houska, J. Kalal, and N. A. Cepalova, "Adsorption of Human Fibrinogen and Human Serus Albumin Onto Polyethylene," Am. Biomed. Eng., 8, 245 (1980).

77. J. L. Brash, and S. Unigal, "Dependence of Albumin-Fibrinogen Simple and Competitive Adsorption on Surface Properties of Biomaterials," J. Polymer Sci.: Polymer Symposium, 66, 377 (1979).

78. S. W. Kim and R. G. Lee, "Adsorption of Blood Proteins onto Polymer Surfaces," Advances in Chemistry Series, No. 145, Applied Chemistry at Protein Interfaces 1975.

79. H. F. P. Purday, An Introduction to the Mechanics of Viscous Flow, Chapt. 2, Dover Publication 1949.

80. R. B. Bind, Transport Phenomena, Chapt. 2, Wiley 1960.

81. W. Lynch, "The Unique Properties of Silicone Rubber," from Handbook of Silicone Rubber Fabrication, Van Nostrand Reinhold, Chapt. 1, 1 (1973).

82. L. M. Smith, "Cell Adhesion to Treated Polymer Surfaces," Ph.D. Thesis, University of Utah, Department of Materials Science and Engineering, June 1979.